DEPARTMENT OF THE AIR FORCE

AIR UNIVERSITY

AIR FORCE INSTITUTE OF TECHNOLOGY

Wright-Patterson Air Force Base, Ohio

AFIT/GA/AA/88D-10

CONTROL SYSTEM FOR MAINTAINING STABLE ORBITS AROUND PHOBOS

THESIS

Mary K. Solomon
Captain, USAF

AFIT/GA/AA/88D-10

Approved for public release; distribution unlimited

AFIT/GA/AA/88D-10

CONTROL SYSTEM FOR MAINTAINING STABLE ORBITS AROUND PHOBOS

THESIS

Presented to the Faculty of the School of Engineering

of the Air Force Institute of Technology

Air University

In Partial Fulfillment of the

Requirements for the Degree of

Master of Science in Astronautical Engineering

Mary K. Solomon, B.S.E.E.

Captain, USAF

December 1988

Acknowledgements

I'd like to thank my advisor, Dr. William Wiesel, for all of his guidance, and also for his "Job-like" patience which enabled me to complete this thesis successfully.

Table of Contents

List of Figures

List of Tables

Notation

$[A(t)]$	Variational matrix
$B(t)$	Control distribution vector
C_n, S_n	Fourier coefficients
D	Distance from Phobos to Mars
d	Distance from Mars to satellite
e, G	Error vectors
$[F(t)]$	Matrix of eigenvectors
f_{ij}^{-1}	Elements of $[F(t)]^{-1}$
$f(X)$	Equations of motion
G	Universal gravitational constant
$g(t)$	Controllability vector
H	Hamiltonian
I_{ii}	Moments of inertia
$[J]$	Matrix of Poincaré exponents
k	Gain
L	Lagrangian
M	Mass
p_i	Generalized momenta
q_i	Generalized coordinates
R	Distance from Phobos to satellite
r	Distance from Phobos differential mass element to satellite
T	Kinetic energy, Period
$u(t)$	Control

V	Potential energy
$\mathcal{V}$	Velocity
$X(t)$	State vector

Greek Notation

$\eta(t)$	Modal variable
λ_i	Eigenvalues
ρ	Distance from center of Phobos to differential mass element
$[\Phi(t,t_o)]$	State transition matrix
ω_i	Poincaré exponents
ω	Phobos orbital rate about Mars
Ω	Phobos rotation rate about its axis

Abstract

Phobos can be modeled as a triaxial ellipsoid in a circular orbit around Mars. The orbital dynamics of a satellite in orbit around Phobos are derived using Hamilton's canonical equations. An algorithm is then developed to find closed orbits for a specified period. Periodic orbits in Phobos' orbital plane have been found to be unstable. A control system is developed using scalar modal control to stabilize the orbit by shifting the unstable Poincaré exponent to the left-half plane.

I. Introduction

There are several moons in the solar system which may be modeled as triaxial ellipsoids. This investigation studies periodic orbits about one such ellipsoid, Phobos.

Hamilton's canonical equations are used to derive the equations of motion for a satellite in orbit around Phobos. A method will be developed to locate periodic orbits in Phobos' orbital plane, and determine their stability. Periodic orbits in Phobos' orbital plane have been shown to be unstable (6: 30), so modal control theory will be used to develop a control system which will stabilize these orbits. Once the control has been implemented, it will be tested to determine how far the satellite may deviate from its nominal trajectory before the control becomes unstable. These results are presented in graphical format.

II. Problem Description

Phobos may be modeled as a triaxial ellipsoid. (See Figure 1.) The coordinate system shown in the figure coincides with Phobos' center of mass. Phobos rotates about it's smallest axis ($\hat{z}$ - out of page), with its longest axis, $\hat{y}$, pointed towards Mars. Therefore, Phobos' rotation rate about its own axis, Ω, equals its rotation rate about Mars, ω (6:2). For this investigation, Phobos' orbit about Mars is taken to be circular with radial distance $|D|$. The satellite's orbit about Phobos is denoted by R. Appendix A contains the needed parameters for Mars and Phobos.

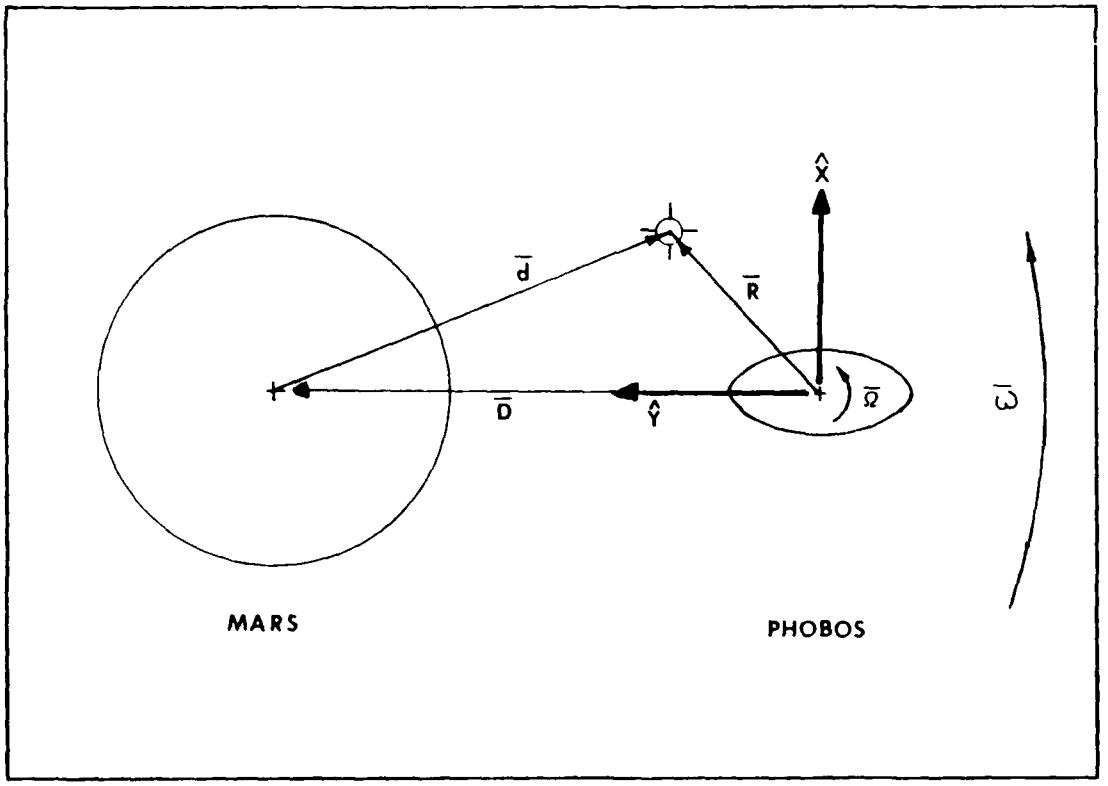

Figure 1 : Coordinate System for Mars and Phobos

Equations of Motion

Hamilton's canonical equations will be used to derive the equations of motion. The Hamiltonian is defined as

$$H = \sum p_i \dot{q}_i - L \tag{2-1}$$

where q_i and p_i are the generalized coordinates and momenta, respectively. L is the Lagrangian and is defined as

$$L = T - V \tag{2-2}$$

where T is the satellite's kinetic energy and V is its potential energy. L, and therefore T and V, must be derived in order to assemble the Hamiltonian.

Kinetic Energy The kinetic energy of a satellite with mass, M_{sat}, is defined to be

$$T = \frac{1}{2} M_{sat} \overset{z}{\mathcal{V}}_{sat} \tag{2-3}$$

where $\mathcal{V}_{sat}$ is the velocity of the satellite measured with respect to an inertial frame. Using the center of Mars as the inertial reference results in

$$\overset{z}{\mathcal{V}}_{sat} = \dot{d} \cdot \dot{d} \tag{2-4}$$

where $\dot{d}$ is the time rate of change of d with respect to the inertial frame. Using Figure 1, $\dot{d}$ may be written as

$$\dot{d} = \dot{R} - \dot{D} \tag{2-5}$$

where $\dot{D}$ is the time derivative of D with respect to the inertial frame and may be expressed as

$$\dot{D} = \dot{D}_{rel} + \vec{\omega} \times D \tag{2-6}$$

The first term in Equation (2-6) is the time derivative of D with respect to the rotating frame. Since Phobos is in a circular orbit about Mars, this term is equal to zero. Therefore,

$$\dot{D} = \vec{\omega} \times D = \omega\hat{z} \times D\hat{y} = -\omega D\hat{x} \tag{2-7}$$

Since ω and Ω are equal

$$\dot{D} = -\Omega D\hat{x} \tag{2-8}$$

Likewise, $\dot{R}$, the time derivative of R with respect to the inertial frame, may be written

$$\dot{R} = R_{rel} + \vec{\Omega} \times R \tag{2-9}$$

If R is defined to be

$$R = X\hat{x} + Y\hat{y} + Z\hat{z} \tag{2-10}$$

then

$$\dot{\mathbf{R}} = (\dot{X}\hat{x} + \dot{Y}\hat{y} + \dot{Z}\hat{z}) + (\Omega X\hat{y} - \Omega Y\hat{x}) \qquad (2\text{–}11)$$

Combining Equations (2–5), (2–8), and (2–11) results in

$$\dot{\mathbf{d}} = (\dot{X} - \Omega Y + \Omega D)\hat{x} + (\dot{Y} + \Omega X)\hat{y} + \dot{Z}\hat{z} \qquad (2\text{–}12)$$

Now, the expression for kinetic energy

$$T = \frac{1}{2} M_{sat}\, \dot{\mathbf{d}}\cdot\dot{\mathbf{d}} \qquad (2\text{–}13)$$

may be written using Equation (2–12) as

$$T = \frac{1}{2} M_{sat}\left[(\dot{X} - \Omega Y + \Omega D)^2 + (\dot{Y} + \Omega X)^2 + \dot{Z}^2\right] \qquad (2\text{–}14)$$

Potential Energy The potential energy of the satellite is the sum of the potential energies due to Mars and to Phobos

$$V_{sat} = V_{mars} + V_{phob} \qquad (2\text{–}15)$$

Potential Energy Due to Mars The potential energy of the satellite due to the gravitational attraction of Mars is

$$V_{mars} = -\frac{GM_{mars}M_{sat}}{d} \qquad (2\text{–}16)$$

where G is the Universal Gravitational Constant. The magnitude, d, may be written

$$d^{-1} = |\mathbf{R}-\mathbf{D}|^{-1} = \left(R^2 - 2\mathbf{R}\cdot\mathbf{D} + D^2\right)^{-1/2} \qquad (2\text{–}17)$$

the binomial expansion of which may be shown to be

$$d^{-1} = \frac{1}{D}\left[1 + \frac{DY}{D^2} - \frac{R^2}{2D^2} - \frac{3}{8}\left[\frac{2DY - R^2}{D^2}\right]^2\right] \qquad (2\text{–}18)$$

Since D » R, the higher order terms of the expansion are negligible and may be ignored. Substituting Equation (2–18) in Equation (2–16) provides an expression for the potential due to Mars

$$V_{mars} = -\frac{GM_{mars}M_{sat}}{D}\left[1 + \frac{DY}{D^2} - \frac{R^2}{2D^2} - \frac{3}{8}\left[\frac{2DY - R^2}{D^2}\right]^2\right] \qquad (2\text{–}19)$$

Potential Energy Due to Phobos The gravitational potential for an arbitrary body is derived by Meirovitch (5: 430-436) and will be used to develop an expression for the satellites potential due to Phobos. Figure 2 shows the coordinate system that will be used for this development. The integral form of gravitational potential energy is

$$V_{phob} = -GM_{sat}\int\frac{dM_{phob}}{r} \qquad (2\text{–}20)$$

where

$$r^{-1} = |\bar{R} - \bar{\rho}|^{-1} = \left(R^2 - 2\bar{R}\cdot\bar{\rho} + \rho^2 \right)^{1/2} \qquad (2\text{–}21)$$

Doing another binomial expansion results in

$$r^{-1} = R^{-1} + \frac{\bar{R}\cdot\bar{\rho}}{R^3} - \frac{\rho^2}{2R^3} + \frac{3(\bar{R}\cdot\bar{\rho})^2}{2R^5} - \mathcal{O}\left(\frac{\rho^3}{R^5} \right) \qquad (2\text{–}22)$$

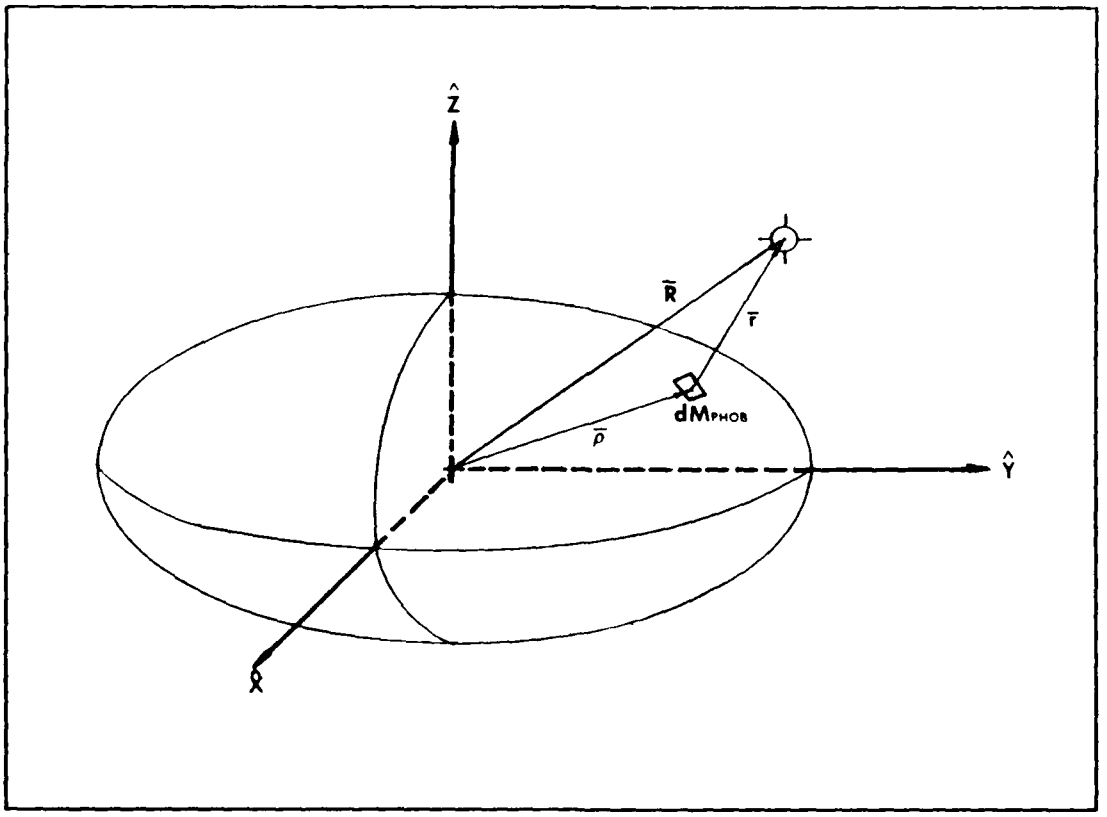

Figure 2: Gravitational Potential Due to Phobos

The terms of Order $\left[\frac{\rho^3}{R^3} \right]$ and above in Equation (2–22) will be dropped so that the equations of motion will be a system of linear differential equations. Using the following definitions for $\bar{\rho}$ and R

$$\bar{\rho} = a\hat{x} + b\hat{y} + c\hat{z} \qquad (2\text{–}23a)$$

$$R = X\hat{x} + Y\hat{y} + Z\hat{z} \qquad (2\text{–}23b)$$

and after some algebraic manipulation, Equations (2–22) and (2–20) may be combined to give

$$V_{phob} = -\frac{GM_{sat}}{R}\int dM_{phob} - \frac{GM_{sat}}{R^3}\int \left[aX + bY + cZ\right] dM_{phob}$$

$$-\frac{GM_{sat}}{2R^3}\int \left[\frac{3}{R^2}(aX + bY + cZ)^2 - (a^2 + b^2 + c^2)\right] dM_{phob} \qquad (2\text{–}24)$$

Evaluating the first integral in Equation (2–24) gives

$$-\frac{GM_{sat}}{R}\int dM_{phob} = -\frac{GM_{sat}M_{phob}}{R} \qquad (2\text{–}25)$$

The second integral in Equation (2–24) goes to zero when the origin of the axis system is placed at the center of mass.

The third integral in Equation (2–24) may be expanded

$$\frac{GMeat}{2R^3}\int\left[\frac{3}{R^2}(aX+bY+cZ)^2-(a^2+b^2+c^2)\right]dMphob =$$

$$\frac{GMeat}{2R^3}\left\{\left[\frac{3X^2}{R^2}-1\right]\int a^2dMphob + \left[\frac{3Y^2}{R^2}-1\right]\int b^2dMphob\right.$$

$$+\left[\frac{3Z^2}{R^2}-1\right]\int c^2dMphob + \frac{6XY}{R^2}\int ab\ dMphob$$

$$\left.+\frac{6XZ}{R^2}\int ac\ dMphob + \frac{6YZ}{R^2}\int bc\ dMphob\right. \qquad (2-26)$$

By using definitions for mass moments of inertia (Ixx, Iyy, Izz) and mass products of inertia (Ixy, Ixz, Iyz), the terms of Equation (2-26) may be simplified

$$\int a^2\, dMphob = \frac{1}{2} \int \left[(a^2 + b^2) + (a^2 + c^2) - (b^2 + c^2)\right] dMphob$$

$$= \frac{1}{2} (Izz + Iyy - Ixx)$$

$$\int b^2\, dMphob = \frac{1}{2} \int \left[(a^2 + b^2) + (b^2 + c^2) - (a^2 + c^2)\right] dMphob$$

$$= \frac{1}{2} (Izz + Ixx - Iyy)$$

$$\int c^2\, dMphob = \frac{1}{2} \int \left[(a^2 + c^2) + (b^2 + c^2) - (a^2 + b^2)\right] dMphob$$

$$= \frac{1}{2} (Iyy + Ixx - Izz)$$

(2-27)

$$\int ab\, dMphob = Ixy$$

$$\int ac\, dMphob = Ixz$$

$$\int bc\, dMphob = Iyz$$

If the axes are arranged such that they align with the principle axes of Phobos, then the products of inertia are zero. Equation (2-26) may now be rewritten

$$V_{phob} = -\frac{GM_{sat}M_{phob}}{R}$$

$$-\frac{GM_{sat}M_{phob}}{4R^3}\left[\left(\frac{3X^2}{R^2}-1\right)(I_{yy}+I_{zz}-I_{xx})\right.$$

$$+\left(\frac{3Y^2}{R^2}-1\right)(I_{xx}+I_{zz}-I_{yy})$$

$$\left.+\left(\frac{3Z^2}{R^2}-1\right)(I_{xx}+I_{yy}-I_{zz})\right] \qquad (2\text{-}28)$$

which further simplifies to

$$V_{phob} = -\frac{GM_{sat}M_{phob}}{R}+\frac{GM_{sat}}{4R^3}(I_{xx}+I_{yy}+I_{zz})$$

$$-\frac{3GM_{sat}}{4R^5}\left[X^2(I_{yy}+I_{zz}-I_{xx})+\right.$$

$$\left.Y^2(I_{xx}+I_{zz}-I_{yy})+Z^2(I_{xx}+I_{yy}-I_{zz})\right] \qquad (2\text{-}29)$$

Hamiltonian Mechanics Since expressions for both the kinetic and potential energies have been developed, the Lagrangian may be formed. For convenience, the mass of the satellite will be divided out, and the equations developed will be on a per unit mass basis. Substituting Equations (2–29), (2–19), and (2–14) into Equation (2–2) gives a Lagrangian

$$L = \frac{1}{2}\left[(\dot{X} + \Omega(D - Y))^2 + (\dot{Y} + \Omega X)^2 + \dot{Z}^2 \right]$$

$$+ \frac{GM_{mars}}{D}\left[1 + \frac{DY}{D^2} - \frac{R^2}{2D^2} - \frac{3}{8}\left(\frac{2DY - R^2}{D^2}\right)^2 \right]$$

$$+ \frac{GM_{phob}}{R} - \frac{G}{4R^3}(I_{xx} + I_{yy} + I_{zz})$$

$$+ \frac{3G}{4R^5}\left[X^2(I_{yy} + I_{zz} - I_{xx}) \right.$$

$$\left. + Y^2(I_{xx} + I_{zz} - I_{yy}) + Z^2(I_{xx} + I_{yy} - I_{zz}) \right] \qquad (2-30)$$

Before the Hamiltonian

$$H = P_x\dot{X} + P_y\dot{Y} + P_z\dot{Z} - L \qquad (2-31)$$

may be formed, expressions for the generalized velocities are needed. This is accomplished by using Lagrange's equations

$$P_x = \frac{\partial L}{\partial \dot{X}} = \dot{X} + \Omega(D - Y) \qquad (2-31a)$$

$$P_y = \frac{\partial L}{\partial \dot{Y}} = \dot{Y} + \Omega X \qquad (2-31b)$$

$$P_z = \frac{\partial L}{\partial \dot{Z}} = \dot{Z} \qquad (2-31c)$$

which allow the Lagrangian to be simplified to

$$L = \frac{1}{2}\left[P_x^2 + P_y^2 P_z^2 \right]$$

$$+ \frac{GM_{mars}}{D}\left[1 + \frac{DY}{D^2} - \frac{R^2}{2D^2} - \frac{3}{8}\left(\frac{2DY - R^2}{D^2}\right)^2 \right]$$

$$+ \frac{GM_{phob}}{R} - \frac{G}{4R^3}(I_{xx} + I_{yy} + I_{zz})$$

$$+ \frac{3G}{4R^5}\left[X^2(I_{yy} + I_{zz} - I_{xx}) + Y^2(I_{xx} + I_{zz} - I_{yy}) \right.$$

$$\left. + Z^2(I_{xx} + I_{yy} - I_{zz}) \right] \qquad (2\text{–}33)$$

This allows Equation (2–31) to be rewritten as

$$H = P_x\left[P_x + \Omega(Y - D)\right] + P_y\left[P_y - \Omega X\right] + P_z^2 - L \qquad (2\text{–}34)$$

The Hamiltonian may now be presented in its final form

$$H = \frac{1}{2}\left[P_x^2 + P_y^2 + P_z^2 \right] + P_x\Omega(Y - D) - P_y\Omega X$$

$$- \frac{GM_{mars}}{D}\left[1 + \frac{DY}{D^2} - \frac{R^2}{2D^2} - \frac{3}{8}\left[\frac{2DY - R^2}{D^2}\right]^2 \right]$$

$$- \frac{GM_{phob}}{R} + \frac{GI}{4R^3} - \frac{3G}{4R^5}\left[X^2(I - 2I_{xx}) + \right.$$

$$\left. Y^2(I - 2I_{yy}) + Z^2(I - 2I_{zz}) \right] \qquad (2\text{-}35)$$

where $I = I_{xx} + I_{yy} + I_{zz}$. Finally, the equations of motion may be formed

$$\dot{X} = \frac{\partial H}{\partial P_x} = P_x + \Omega(Y - D) \qquad (2\text{-}36a)$$

$$\dot{Y} = \frac{\partial H}{\partial P_x} = P_y - \Omega X \qquad (2\text{-}36b)$$

$$\dot{Z} = \frac{\partial H}{\partial P_z} = P_z \qquad (2\text{-}36c)$$

$$\dot{P}_x = -\frac{\partial H}{\partial X} = \Omega P_y - \frac{GM_{mars}}{D}\left[\frac{X}{D^2} - \frac{3XY}{D^3} - \frac{3R^2X}{2D^4}\right] - \frac{GM_{phob}X}{R^3}$$

$$+ \frac{3GIX}{4R^5} - \frac{3GX}{4R^7}\Big[(5X^2 - 2R^2)(I - 2I_{xx})$$

$$+ 5Y^2(I - I_{yy}) + 5Z^2(I - I_{zz})\Big] \qquad (2\text{-}36d)$$

$$\dot{P}_y = -\frac{\partial H}{\partial Y} = -\Omega P_x - \frac{GM_{mars}}{D}\left[\frac{1}{D} - \frac{4Y}{D^2}\,\frac{3(YR^2 - DR^2 - 2DY^2)}{2D^4}\right]$$

$$- \frac{GM_{phob}Y}{R^3} + \frac{3GIY}{4R^5} - \frac{3GY}{4R^7}\Big[5X^2(I - 2I_{xx})$$

$$+ (5Y^2 - 2R^2)(I - I_{yy}) + 5Z^2(I - I_{zz})\Big] \qquad (2\text{-}36e)$$

$$\dot{P}_z = -\frac{\partial H}{\partial Z} = -\frac{GM_{mars}}{D}\left[\frac{Z}{D^2} - \frac{3YZ}{D^3} - \frac{3R^2Z}{2D^4}\right] - \frac{GM_{phob}Z}{R^3}$$

$$+ \frac{3GIZ}{4R^5} - \frac{3GZ}{4R^7}\Big[5X^2(I - 2I_{xx})$$

$$+ 5Y^2(I - I_{yy}) + (5Z^2 - 2R^2)(I - I_{zz})\Big] \qquad (2\text{-}36f)$$

These are the equations of motion for this system. They are also listed in Appendix B for convenience.

III. Periodic Orbits

The equations of motion may now be integrated with selected initial conditions in an attempt to locate periodic orbits. If the initial conditions do not produce a closed orbit, the equations are reintegrated with new conditions until a closed orbit is found. To prevent arbitrary selection of initial conditions, an algorithm is required which will systematically alter the initial conditions until the desired orbit is found. But, before the algorithm is developed, it would be beneficial to know in what way the orbit trajectory is altered when the initial conditions are changed. There exists a method (8: 112-114) to obtain this information which will be described here for completeness.

State Transition Matrix

The equations of motion may be represented as

$$\dot{\mathbf{X}} = \mathbf{f}(\mathbf{X}) \tag{3-1}$$

where $\mathbf{X}$ and $\mathbf{f}(\mathbf{X})$ are vectors whose elements are

$$\mathbf{X} = \begin{Bmatrix} X \\ Y \\ Z \\ P_x \\ P_y \\ P_z \end{Bmatrix} \qquad \mathbf{f}(\mathbf{X}) = \begin{Bmatrix} \text{Eqn 2-36a} \\ \text{Eqn 2-36b} \\ \text{Eqn 2-36c} \\ \text{Eqn 2-36d} \\ \text{Eqn 2-36e} \\ \text{Eqn 2-36f} \end{Bmatrix} \tag{3-2}$$

If a set of initial conditions result in a trajectory, $X_o(t)$, then a nearby trajectory may be represented by

$$X(t) = X_o(t) + \delta X(t) \tag{3-3}$$

where δX is a small deviation from the initial trajectory. Substituting this trajectory into the equations of motion results in

$$\dot{X}(t) = \dot{X}_o(t) + \delta\dot{X}(t) = f(X + \delta X) \tag{3-4}$$

Expanding Equation (3-4) in a Taylor series about the initial trajectory (ie, about $\delta X = 0$) produces

$$\dot{X}_o + \delta\dot{X} = f(X_o) + \left.\frac{\partial f}{\partial X}\right|_{X_o} \delta X + \ldots \tag{3-5}$$

Using Equation (3-1) (and dropping higher order terms), this may be simplified to

$$\delta\dot{X} = \left.\frac{\partial f}{\partial X}\right|_{X_o} \delta X \tag{3-6}$$

This system of equations is called the equations of variation and is often written

$$\delta\dot{X} = [A]\delta X \tag{3-7}$$

where [A], the variational matrix, is defined as

$$[A(t)] = \left.\frac{\partial f}{\partial X}\right|_{x_o} \qquad (3\text{–}8)$$

The elements of [A(t)] may be found in Appendix C.

Equation (3–7) is a linear set of equations and, therefore, has a fundamental solution set of six independent solutions, ϕ_i, whose initial conditions are $\phi_{ij} = \delta_{ij}$. The Kroenecker Delta, δ_{ij}, equals one when $i = j$ and zero when $i \neq j$. A general solution to Equation (3–7) may be written

$$\delta X(t) = \sum \phi_{ij}(t)\ \delta X_j(t_o) \qquad j = 1\text{–}6 \qquad (3\text{–}9)$$

In matrix form, this may be written

$$\delta X(t) = \Phi(t,t_o)\delta X(t_o) \qquad (3\text{–}10)$$

where $\Phi(t,t_o)$, the state transition matrix, is a square matrix with columns made of ϕ_i. It relates the variations at time t to changes in the initial conditions. Taking the derivative of Equation (3–10), substituting into Equation (3-7), and making the appropriate cancellations results in

$$\dot{\Phi}(t,t_o) = [A]\Phi(t,t_o) \qquad (3\text{–}11)$$

Hence, numerical integration of the equations of motion propagates the reference trajectory; numerical integration of Equation (3-11) along with the equations of motion also propagates the displaced trajectories caused by different initial conditions.

Locating Periodic Orbits

Since information is now available on how the initial conditions affect the orbit trajectory, a method may be developed to determine the proper initial conditions which will produce a closed orbit for a given period.

First, an initial estimate for the initial conditions is needed to integrate the equations of motion. In this case, the initial conditions may be obtained from circular orbit calculations (taking into account the rotating reference frame.)

Second, the equations of motion and variation will be integrated for a specified amount of time.

Third, if the orbit does not close after one period, then the initial conditions should be altered, and the equations reintegrated, until a periodic orbit is found. Corrections to the initial conditions will be determined using a method described by Wiesel (8:117-121).

Figure 3 shows part of an orbit starting on the y-axis and continuing for half a period. For orbits limited to perpendicular crossings of the y axis in Phobos' orbital

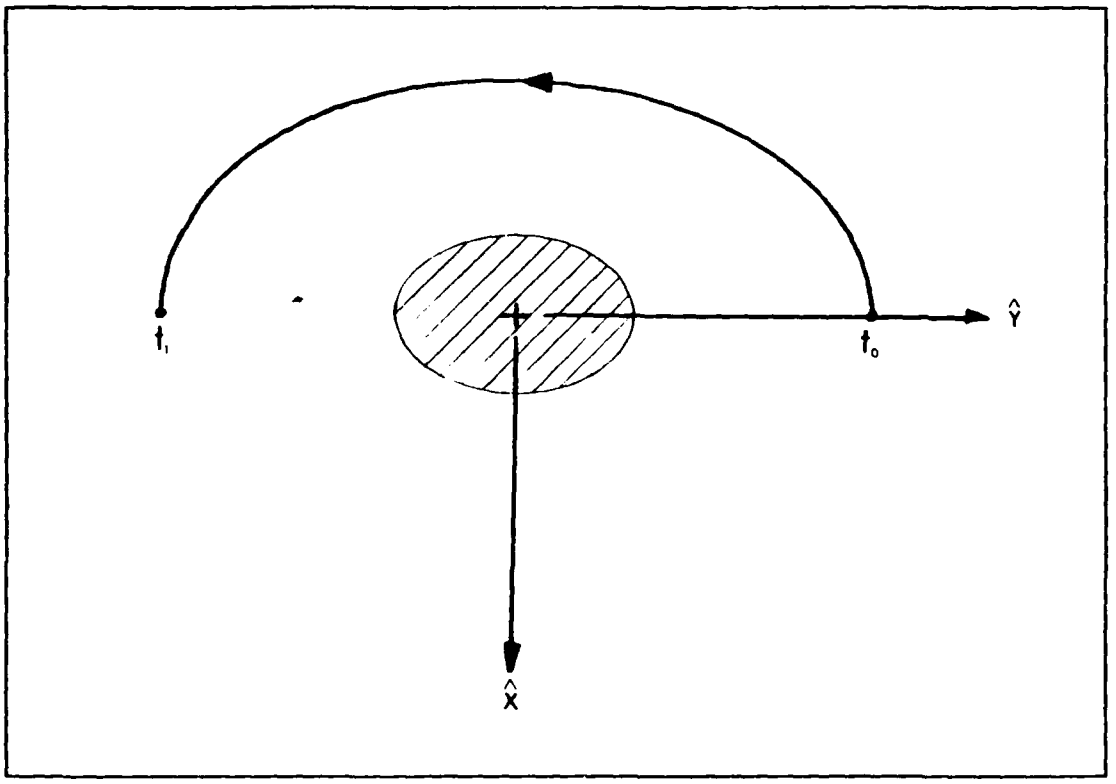

Figure 3: Periodic Orbit Symmetry

plane, symmetry allows certain conditions to hold true. These conditions are used to define a vector, G, such that

$$G = \begin{bmatrix} X(t_1) \\ P_y(t_1) \\ P_z(t_1) \end{bmatrix} = 0 \qquad (3\text{–}12)$$

If G is evaluated on a reference trajectory which is not a periodic orbit, then G will not be zero. It will be an error vector, e. The smaller e is, the closer the trajectory is to a periodic orbit. For orbits that deviate

from the reference trajectory, $X_o(t)$, G may be rewritten using a Taylor series expansion about $X_o(t)$

$$G\left[X_o(t_1) + \delta X(t_1),\ t_1\right] = G\left[X(t_1),\ t_1\right] + [B]\delta X(t_1) + \ldots \tag{3-13}$$

where

$$[B] = \left.\frac{\partial G}{\partial X}\right|_{X_o(t_1)} = \begin{bmatrix} 1 & 0 & 0 & 0 & 0 \\ 0 & 0 & 0 & 1 & 0 \\ 0 & 0 & 0 & 0 & 1 \end{bmatrix} \tag{3-14}$$

If the deviated orbit is actually the desired periodic orbit, then

$$G\left[X_o(t_1) + \delta X(t_1),\ t_1\right] = 0 \tag{3-15}$$

For the reference trajectory, as indicated,

$$G\left[X(t_1),\ t_1\right] = e \tag{3-16}$$

Equation (3-13) may now be rewritten

$$-e = [B]\delta X(t_1) \tag{3-17}$$

What is needed, however, is a relationship between the error and the change in initial conditions. This may be

accomplished by using the state transition matrix. Equation (3–10) may be substitued into Equation (3–17) to give

$$-e = [B]\Phi(t_1,t_o)\delta X(t_o) \tag{3–18}$$

Solving for $\delta X(t_o)$ requires the product $[B]\Phi(t_1,t_o)$ to be inverted; however, the product is not invertable because it is a 3 x 6 matrix. Yet, examination of the product reveals

$$[B]\Phi(t_1,t_o)\delta X(t_o) = [B]\Phi(t_1,t_o) \begin{Bmatrix} \delta X(t_o) \\ \delta Y(t_o) \\ \delta Z(t_o) \\ \delta P_x(t_o) \\ \delta P_y(t_o) \\ \delta P_z(t_o) \end{Bmatrix} \tag{3–19}$$

Because of the way the problem has been set up, the initial conditions for X, P_y, and P_z are not allowed to vary, and $\delta X = \delta P_y = \delta P_z = 0$. Therefore, the corresponding rows of the product $[B]\Phi$ may be eliminated. Equation (3–19) may be rewritten

$$[B]\Phi(t_1,t_o)\delta X(t_o) = \left[[B]\Phi(t_1,t_o)\right]_{234} \begin{Bmatrix} \delta y(t_o) \\ \delta Z(t_o) \\ \delta P_x(t_o) \end{Bmatrix} \tag{3–20}$$

Equation (3–18) may now be solved for $\delta X(t_o)$, resulting in

$$\begin{Bmatrix} \delta y(t_o) \\ \delta Z(t_o) \\ \delta P_x(t_o) \end{Bmatrix} = - \left[[B] \Phi(t_1, t_o) \right]^{-1}_{2\times 4} e \qquad (3\text{–}21)$$

The initial conditions may now be corrected with Equation (3–21), and the equations of motion and variation reintegrated. This process is continued until the elements of G are at an accepted tolerance.

Verification of Equations

Before a periodic solution may be found, the equations of motion and variation must be calculated and programed correctly.

Equations of Motion The Hamiltonian for this system is not a function of time and should remain constant through out the integration. Therefore, the Hamiltonian at different points along the orbit may be compared. If they differ, then the equations of motion may not be correct. In order to locate where the problem may lie, different components may be "turned off" (e.g., by setting the mass of Mars to zero) or they may be "turned up" (e.g., by increasing the moments of inertia for Phobos). By varying the parameters and observing how the Hamiltonian is affected, the error in the equations may be found.

If the Hamiltonian remains constant during part of the trajectory, then "jumps" to a new value (and remains constant at this new value), the trajectory has passed too close to a singularity. The trajectory which results is not reliable and, therefore, the equations should be reintegrated with different initial conditions.

Equations of Variation The variational matrix may be verified by using its definition

$$[A(t)] = \left.\frac{\partial f}{\partial X}\right|_{X_o} \qquad (3\text{–}22)$$

Using an approximation for the derivative

$$[A] = \frac{f(X + \Delta X) - f(X)}{\Delta X} \qquad (3\text{–}23)$$

where ΔX is a small number. Each column of [A] will be checked by varying the corresponding element of X.

State Transition Matrix The state transition matrix may be verified by noting

$$\Phi(t,t_o) = \left.\frac{\partial X}{\partial X_o}\right|_{X_o} \qquad (3\text{–}24)$$

Using an approximation for the derivative

$$\Phi(t,t_o) = \frac{X_2(t) - X_1(t)}{\Delta X_o} \qquad (3\text{–}25)$$

where ΔX_o is a small change in the initial condition. $X_1(t)$ is the state at time t started from initial condition X_o, and $X_2(t)$ is the state at time t started from initial condition, $X_o + \Delta X_o$. Each column of $\Phi(t,t_o)$ will be checked by varying the corresponding element of X_o.

IV. Stability and Control

Once a periodic orbit has been located, the next step is to determine if it is stable. In other words: If a satellite is placed in a periodic orbit, will it remain in that orbit (even if it experiences minor perturbations?) If the orbit is inherently unstable, then a control system needs to be implemented to ensure stability (2: 671-676).

Stability of Orbits

The system of equations

$$\dot{\delta X} = [A(t)]\delta X \tag{4-1}$$

is time periodic and linear. The solution for time periodic, linear systems was discovered by Floquet. The most common application of Floquet theory is to determine the stability of periodic orbits.

As discussed previously, a solution to Equation (4-1) is given by

$$\delta X(t) = \Phi(t,t_o)\delta X(t_o) \tag{4-2}$$

where $\Phi(t,t_o)$ is calculated by

$$\dot{\Phi}(t,t_o) = [A(t)]\Phi(t,t_o) \tag{4-3}$$

with the initial condition for $\Phi(t,t_o)$ being [I], the identity matrix. Floquet's theorem states that the state transition matrix may be factored such that

$$\Phi(t,t_o) = [F(t)]\, \exp\{[J]t\}\, [F(t_o)]^{-1} \qquad (4-4)$$

[J], a constant matrix usually in the Jordan normal form, has diagonal entries called Poincaré exponents which are labeled ω_i. They are analogous to the eigenvalues of a constant coefficient system. The matrix [F(t)] is a time periodic matrix with the same period, T, as the original system. Therefore, [F(T)] = [F(0)] and Equation (4-4) may be written

$$\Phi(T,0) = [F(0)]\, \exp\{[J]T\}\, [F(0)]^{-1} \qquad (4-5)$$

If Equation (4-5) is rewritten as

$$\exp\{[J]T\} = [F(0)]^{-1}\Phi(T,0)\, [F(0)] \qquad (4-6)$$

it shows that [F(0)] is the matrix of eigenvectors of $\Phi(T,0)$. The eigenvalues, λ_i, of $\Phi(T,0)$ are related to the Poincaré exponents by

$$\lambda_i = \exp\{\omega_i T\} \tag{4-7}$$

or

$$\omega_i = (1/T)\ln\lambda_i \tag{4-8}$$

In order to determine stability, Equation (4-3) is integrated for one period to obtain $\Phi(T,0)$. The Poincaré exponents are then calculated; if any of them have positive real parts, the system is unstable.

Calculating $[F(t)]^{-1}$

The control system for this problem (to be developed later) will require $[F(t)]^{-1}$ to be known at any point in time. Differentiating $[F(t)][F(t)]^{-1} = [I]$ produces

$$[\dot{F}(t)][F(t)]^{-1} + [F(t)][\dot{F}(t)]^{-1} = [0] \tag{4-9}$$

Solving for $[\dot{F}(t)]^{-1}$

$$[\dot{F}(t)]^{-1} = -[F(t)]^{-1}[\dot{F}(t)][\dot{F}(t)]^{-1} \tag{4-10}$$

An expression for $[\dot{F}(t)]$ is now needed. Taking the derivative of Equation (4-4) gives

$$\dot{\Phi}(t,t_o) = [\dot{F}(t)]\, e^{[J]t}\, [F(t_o)]^{-1} + [F(t)][J]\, e^{[J]t}\, [F(t_o))]^{-1} \tag{4-11}$$

Substituting Equations (4-11) and (4-4) into Equation (4-3) and rearranging produces

$$[\dot{F}(t)] = [A(t)][F(t)] - [F(t)][J] \qquad (4\text{-}12)$$

Substitution of Equation (4-12) into (4-10) yields an expression for $[\dot{F}(t)]^{-1}$

$$[\dot{F}(t)]^{-1} = [J][F(t)]^{-1} - [F(t)]^{-1}[A(t)] \qquad (4\text{-}13)$$

Integration of Equation (4-12) over one period will produce values for $[F(t)]^{-1}$ for any time, t. The initial condition for $[F(t)]^{-1}$ is the inverse of the matrix of eigenvectors of $\Phi(T,0)$.

The Poincaré exponents and eigenvalues for the system may be complex, but may be manipulated to produce real matrices for both [J] and [F(t)]. [F(t)] is arranged with the eigenvectors, F_i, as its columns. If F_i is complex (and hence F_{i+1} is its complex conjugate), then the i^{th} column of [F(t)] will be the real part of F_i and the $(i+1)^{th}$ column will be the imaginary part of F_i.

[J] will be arranged in a block diagonal form. If ω_i is real, it will be a diagonal element of [J]. If ω_i is complex (with ω_{i+1} being its complex conjugate), then [J] will have a block diagonal of the form

$$\begin{bmatrix} \mathrm{Re}(\omega_i) & \mathrm{Im}(\omega_i) \\ -\mathrm{Im}(\omega_i) & \mathrm{Re}(\omega_i) \end{bmatrix} \tag{4-14}$$

Since $[F(0)]$ and $[J]$ are now available, Equation (4-13) may be integrated.

A closed form expression is needed to represent $[F(t)]^{-1}$ so that its value at any time will be available. Since $[F(t)]^{-1}$ is periodic, each of its elements, f_{ij}^{-1}, may be written as a Fourier series

$$f_{ij}^{-1} = \frac{1}{2} C_o + C_1\cos(t) + C_2\cos(2t) + \ldots + \frac{1}{2} C_n\cos(nt)$$

$$+ S_1\sin(t) + S_2\sin(2t) + \ldots + S_n\sin(nt) \tag{4-15}$$

where the coefficients are calculated by

$$C_k = \frac{1}{n}\sum_{l=o}^{2n-1} f_{ij}^{-1}(l\alpha)\cos(kl\alpha), \qquad k = 0,1,2,\ldots,n$$

$$S_k = \frac{1}{n}\sum_{l=o}^{2n-1} f_{ij}^{-1}(l\alpha)\sin(kl\alpha), \qquad k = 0,1,\ldots,n-1 \tag{4-16}$$

where $\alpha = 2\pi/2n$ (1: 109). Therefore, numerically finding 2n values of $[F(t)]^{-1}$ spaced over equal time intervals, and using those values in Equations (4-16) and (4-15) will provide an expression for $[F(t)]^{-1}$.

Control

Modal Variables A new variable is now introduced by

$$\delta X(t) = [F(t)]\,\eta(t) \tag{4-17}$$

where $\eta(t)$ is the modal coordinate vector. Taking the derivative of the above expression, and rearranging, produces

$$\dot{\eta}(t) = [F(t)]^{-1}\left[\,\delta\dot{X}(t) - [\dot{F}(t)]\eta(t)\,\right] \tag{4-18}$$

Substitution of Equation (4-1) and, consequently, Equation (4-17), results in

$$\dot{\eta}(t) = [F(t)]^{-1}\left[\,[A(t)][F(t)] - [\dot{F}(t)]\,\right]\eta(t) \tag{4-19}$$

Using Equation (4-12) reduces this to

$$\dot{\eta}(t) = [J]\eta(t) \tag{4-20}$$

Therefore, $[F(t)]$ is a periodic transformation which transforms a periodic system of equations to a constant coefficient system.

Modal Control Theory The Poincaré exponents for the system may be changed by adding feedback

$$\delta\dot{X}(t) = [A(t)]\delta X(t) + B(t)u(t) \tag{4-21}$$

where B(t) is a vector that determines the distribution of control. For this investigation, B(t) is considered constant and given by

$$B = \begin{Bmatrix} 0 \\ 0 \\ 0 \\ 1 \\ 0 \\ 0 \end{Bmatrix} \tag{4-22}$$

which adds the control to the $\dot{P}_x$ direction. Equation (4-21) may be rewritten with modal variables as

$$\dot{\eta}(t) = [J]\eta(t) + g(t)u(t) \tag{4-23}$$

g(t), the controllability matrix, is

$$g(t) = [F(t)]^{-1}B = \begin{Bmatrix} f_{14}^{-1} \\ f_{24}^{-1} \\ f_{34}^{-1} \\ f_{44}^{-1} \\ f_{54}^{-1} \\ f_{64}^{-1} \end{Bmatrix} \tag{4-24}$$

where f_{ij}^{-1} represent the individual elements of $[F(t)]^{-1}$. The i^{th} mode of this system may be controlled only if the i^{th} value of g(t) is nonzero.

For this system, only one mode will be unstable and need to be controlled. To control just one mode, u(t) takes the form

$$u(t) = k(t)\eta(t) = \left[\, 0,\ 0,\ldots,\ k_i(t),\ 0 \,\right] \eta(t) \qquad (4\text{–}25)$$

where the unstable modal variable, $\eta_i(t)$, is multiplied by $k_i(t)$. For this investigation, k is considered constant. Equation (4-23) is now rewritten as

$$\dot{\eta}_c(t) = \left[\, [J] + g(t)k \,\right] \eta_c(t) \qquad (4\text{–}26)$$

or as

$$\dot{\eta}_c(t) = \begin{bmatrix} \omega_1 & 0 & 0 & 0 \\ 0 & \omega_2 & 0 & 0 \\ 0 & 0 & kg_i+\omega_i & 0 \\ 0 & 0 & 0 & \omega_n \end{bmatrix} \eta_c(t) \qquad (4\text{–}27)$$

where $\eta_c(t)$ denotes the controlled system. The controlled system has the same Poincaré exponents as the original system except for the i^{th} exponent. A method is now needed to determine k in order to make ω_i any chosen value.

The equation for the unstable mode is

$$\dot{\eta}_{ci}(t) = \left[\, \omega_i + kg_i(t) \,\right] \eta_{ci}(t) \qquad (4\text{–}28)$$

The use of an integrating factor produces a solution to Equation (4-28)

$$\eta_{ci}(t) = \eta_{ci}(0) \exp\left[\int_0^t \left[\omega_i + kg_i(t)\right]dt\right] \qquad (4-29)$$

Since g(t) actually represents one of the elements of $[F(t)]^{-1}$, it is a periodic function, and may be expressed as a Fourier series. It has a constant term, g_{ic}, and a periodic term, $g_{ip}(t)$. This allows Equation (4-29) to be written

$$\eta_{ci}(t) = \eta_{ci}(0) \exp\left[(\omega_i + kg_{ic})t\right] \exp\left[\int_0^t kg_{ip}(t)dt\right] \qquad (4-30)$$

The second exponential is periodic, so the new Poincaré exponent is the argument of the first exponential

$$\omega_{ci} = \omega_i + kg_{ic} \qquad (4-31)$$

where ω_{ci} denotes the controlled Poincaré exponent.

Now that the desired gain has been established, the control needs to be implemented in the physical variables. Using Equations (4-24) and (4-17), the control may be written using physical coordinates as

$$u(t) = k\,[F(t)]^{-1}\delta X(t) \qquad (4\text{–}32)$$

and the controlled system takes the form

$$\delta\dot{X}(t) = \left[\,[A(t)] + Bk[F(t)]^{-1}\,\right]\delta X(t) \qquad (4\text{–}33)$$

Controlling the State When the control system has been implemented and the shift in the unstable Poincaré exponent verified, the next step is to put the control in the equations of motion

$$\dot{X}(t) = f(X) + Bu(t) \qquad (4\text{–}34)$$

Using Equation (4-32) results in

$$\dot{X}(t) = f(X) + Bk[F(t)]^{-1}\left\{\,X(t) - X_{nom}(t)\,\right\} \qquad (4\text{–}35)$$

where $X_{nom}(t)$ is the trajectory of the desired periodic orbit. Therefore, if the current trajectory is the desired orbit, there will be no control term added to the system.

In summary, controlling an unstable orbit requires the following steps:

1. Using the method described in Section III, locate a closed orbit for a specified period, and determine its Poincaré exponents. Assuming the orbit is unstable,

the Fourier series for $[F(t)]^{-1}$ and $X_{nom}(t)$ are also needed.

2. Select a value for ω_{ic} and determine the value of k needed to obtain the shift in Poincaré exponents.

3. Reintegrate the equations of motion and variation using the controlled system, Equation (4-33), and verify that the unstable root has shifted to the desired ω_{ic}.

4. The control is then implemented in the equations of motion using Equation (4-35) where the effect of the control may be seen directly.

V. Results

Periodic Orbits

The equations of motion and variation were programed and verified using the methods described in section III. The algorithm for locating periodic orbits was then programed and debugged.

Many estimates for initial conditions, both for prograde and retrograde orbits, were tried before the program would converge to a set of initial conditions which would produce a closed orbit. However, the family of orbits which resulted were unrealizable orbits because they went through Phobos.

In order to find physically realizable orbits, the following steps were followed:

1. Phobos' moments of inertia were set to zero, thus making Phobos a point mass.
2. A closed orbit which did not pass through Phobos was located.
3. The moments of inertia were then increased a small amount.
4. The algorithm was rerun with the converged values from Step 2 as the initial conditions.
5. Steps 2 through 5 were repeated until a closed orbit was located with the moments of inertial at their normal value.

Using this method, periodic orbits were located which did not pass through Phobos. The initial conditions to which the algorithm converged for three of these orbits are shown in Table I and match the orbits found by Werner (6:23-24). Figure 4 shows Orbit #1, the orbit for which the remainder of the results are presented.

Table I: Initial Conditions for Three Periodic Orbits

Orbit #	Period (sec)	Y(to) (km)	Px(to) (km/sec)
1	8200	14.16398	2.14778
2	8300	14.64673	2.14765
3	8400	15.14859	2.14754

Stability and Control

The eigenvalues, eigenvectors, and Poincaré exponents were calculated next, and are shown in Table II. The first Poincaré exponent is positive; hence, the orbit is unstable. Therefore, modal control (described in Section IV) was used to shift the exponent to the left half plane.

Calculating $[F(t)]^{-1}$ For this investigation, the unstable Poincaré exponent is ω_1; therefore, only the first row of $[F(t)]^{-1}$ will need to be represented by its Fourier series. The Fourier coefficients were calculated using the method described in Section IV, and are listed in Appendix D.

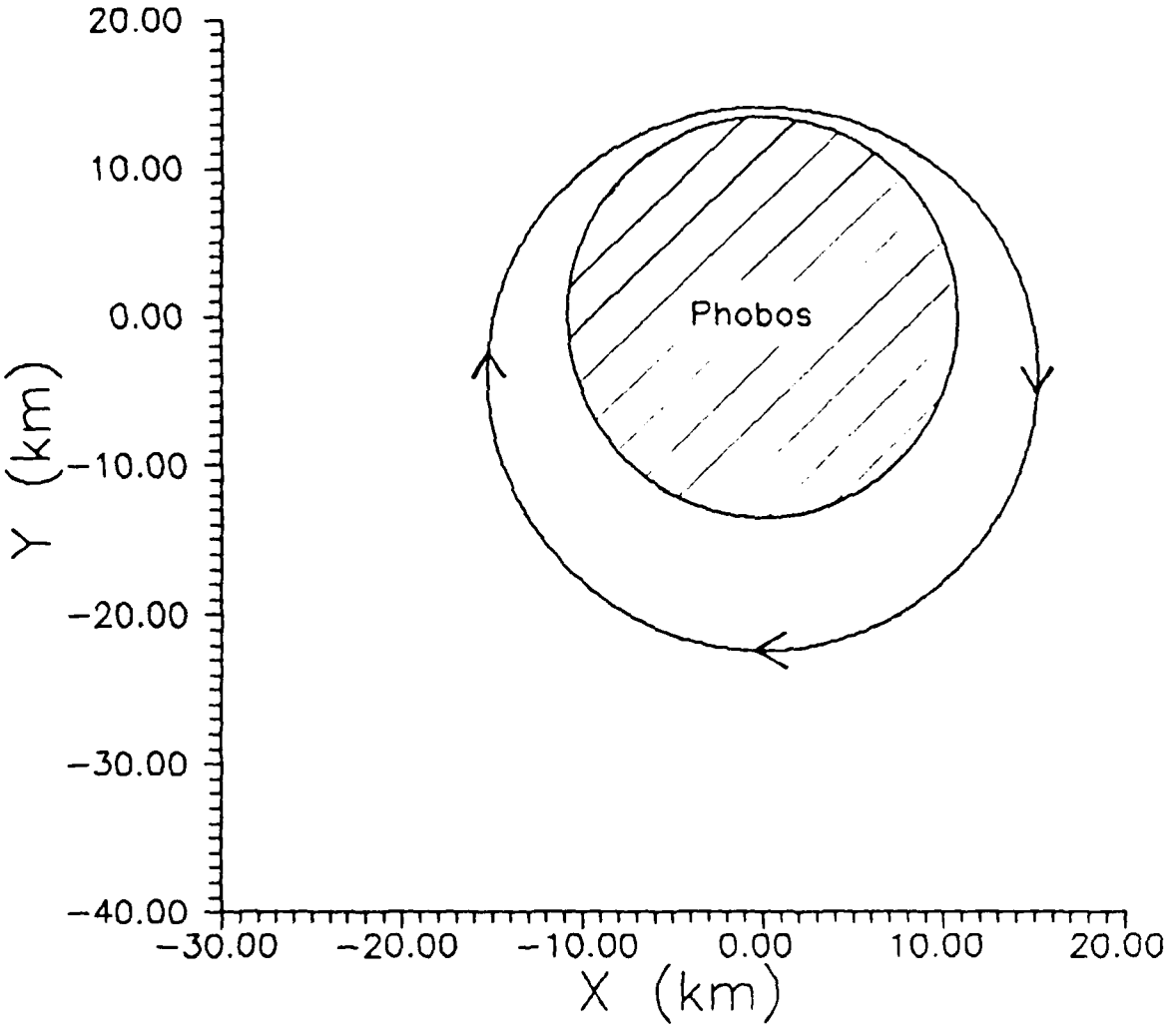

Figure 4: Orbit #1 (Period = 8200 sec)

Note that $[F(0)]^{-1} = [F(T)]^{-1}$, which can be used to verify correct programming and integration of Equation (4-13).

Table II: Eigenvalues (λ), Poincaré Exponents (ω), and Eigenvectors (E) for Orbit #1

$\lambda_1 =$ 3.075e+00 + 0.000e+00 i $\omega_1 =$ 1.370e-04 + 0.000e+00 i	$E_1 =$ [-1.296e+02 + 0.000e+00 i 5.068e+01 + 0.000e+00 i 0.000e+00 + 0.000e+00 i -3.843e-02 + 0.000e+00 i 3.569e-02 + 0.000e+00 i 0.000e+00 + 0.000e+00 i]
$\lambda_2 =$ 3.252e-01 + 0.000e+00 i $\omega_2 =$ -1.370e-04 + 0.000e+00 i	$E_2 =$ [-1.314e+02 + 0.000e+00 i -5.138e+01 + 0.000e+00 i 0.000e+00 + 0.000e+00 i 3.897e-02 + 0.000e+00 i 3.619e-02 + 0.000e+00 i 0.000e+00 + 0.000e+00 i]
$\lambda_3 =$ 1.000e+00 + 3.082e-06 i $\omega_3 =$ 0.000e+00 + 0.000e+00 i	$E_3 =$ [1.623e-01 - 7.758e+03 i -8.840e-03 - 1.974e-07 i 0.000e+00 + 0.000e+00 i 2.434e-06 + 0.000e+00 i -1.231e-04 + 5.884e+00 i 0.000e+00 + 0.000e+00 i]
$\lambda_4 =$ 1.000e+00 - 3.082e-06 i $\omega_4 =$ 0.000e+00 + 0.000e+00 i	$E_4 =$ [1.623e-01 + 7.758e+03 i -8.840e-03 + 1.974e-07 i 0.000e+00 + 0.000e+00 i 2.434e-06 + 0.000e+00 i -1.231e-04 - 5.884e+00 i 0.000e+00 + 0.000e+00 i]
$\lambda_5 =$ -7.988e-01 + 6.016e-01 i $\omega_5 =$ 0.000e+00 + 3.044e-04 i	$E_5 =$ [0.000e+00 + 0.000e+00 i 0.000e+00 + 0.000e+00 i -3.559e+01 + 2.726e+02 i 0.000e+00 + 0.000e+00 i 0.000e+00 + 0.000e+00 i 3.339e-01 + 4.360e-02 i]
$\lambda_6 =$ -7.988e-01 - 6.016e-01 i $\omega_6 =$ 0.000e+00 - 3.044e-04 i	$E_6 =$ [0.000e+00 + 0.000e+00 i 0.000e+00 + 0.000e+00 i -3.559e+01 - 2.726e+02 i 0.000e+00 + 0.000e+00 i 0.000e+00 + 0.000e+00 i 3.339e-01 - 4.360e-02 i]

Modal Control Examination of Equation (4–31) shows

$$\omega_{ci} = \omega_i + kg_{ic} \tag{5–3}$$

where, in this case, the unstable exponent is

$$\omega_i = 1.370e\text{-}04 \tag{5–4}$$

Shifting the unstable exponent to a desired value of

$$\omega_{ci} = -2.000e\text{-}04 \tag{5–5}$$

results in the equation

$$-2.000e\text{-}04 = 1.370e\text{-}04 + kg_{ic} \tag{5–6}$$

g_{ic} is the constant part (the Co Fourier coefficient) of f_{i4}^{-1} (see Equation (4–24)) and is

$$g_{ic} = -14.3244 \tag{5–7}$$

Equation (5–6) may now be solved for k, resulting in

$$k = 2.3526e\text{-}05 \tag{5–8}$$

Equation (4-33) may now be integrated to verify the shift in the Poincaré exponent. The Poincaré exponents for the controlled system are listed in Table III, and match predicted results.

Table III: Poincaré Exponents for the Controlled System

ω_1 = -2.000e-04 + 0.000e+00 i

ω_2 = -1.370e-04 + 0.000e+00 i

ω_3 = 0.000e+00 + 0.000e+00 i

ω_4 = 0.000e+00 + 0.000e+00 i

ω_5 = 0.000e+00 + 3.044e-04 i

ω_6 = 0.000e+00 − 3.044e-04 i

State Control Equation (4-35) may now be used to add the control to the state. Various initial conditions were used to test how the control system reacted to changes in the nominal trajectory. Figure 5 shows the amount of control thrust needed to maintain the nominal orbit when the initial conditions for X were displaced from the nominal value by .5, 10, and 50 meters. The periodic oscillations which appear on the graph are caused by the truncation of the Fourier series for $[F(t)]^{-1}$ and X(t). The sign change for the initial control value may also be explained by the Fourier series truncations. These phenomenon may be more readily observed by plotting the control output for a nominal

trajectory, shown in Figure 6. The small error in the Fourier series representations of $[F(t)]^{-1}$ and X(t) produce a control output, which starts as a positive value and then converges to the same periodic oscillations as do the curves in Figure 5.

When the initial conditions are displaced beyond the linear control region, the control becomes unstable. This is shown in Figure 7. For the X direction, the instability occurs when the displacement exceeds 5 kilometers.

The control thrust was also plotted for initial displacements in Y, P_x, and P_y for both the stable and unstable regions. These graphs are similar to Figures 5 and 7, and are shown in Appendix F. Table IV lists the displacements in X, Y, P_x, P_y which produce unstable control outputs when the control thrust is in the $\dot{P}_x$ direction.

Table IV: Displacements Which Produce Unstable Control in $\dot{P}_x$ Direction

ΔX : 5 km	ΔP_x : .5 cm/sec
ΔY : 10 m	ΔP_y : 1 m/sec

It should also be noted that displacements in Z or P_z are not controllable because $f_{13}^{-1}(t)$ and $f_{14}^{-1}(t)$ are zero for all time (See Equation (4-35)). However, the orbit is already stable in these two modes, as investigation of the Poincaré exponents , ω_3 and ω_4, will reveal.

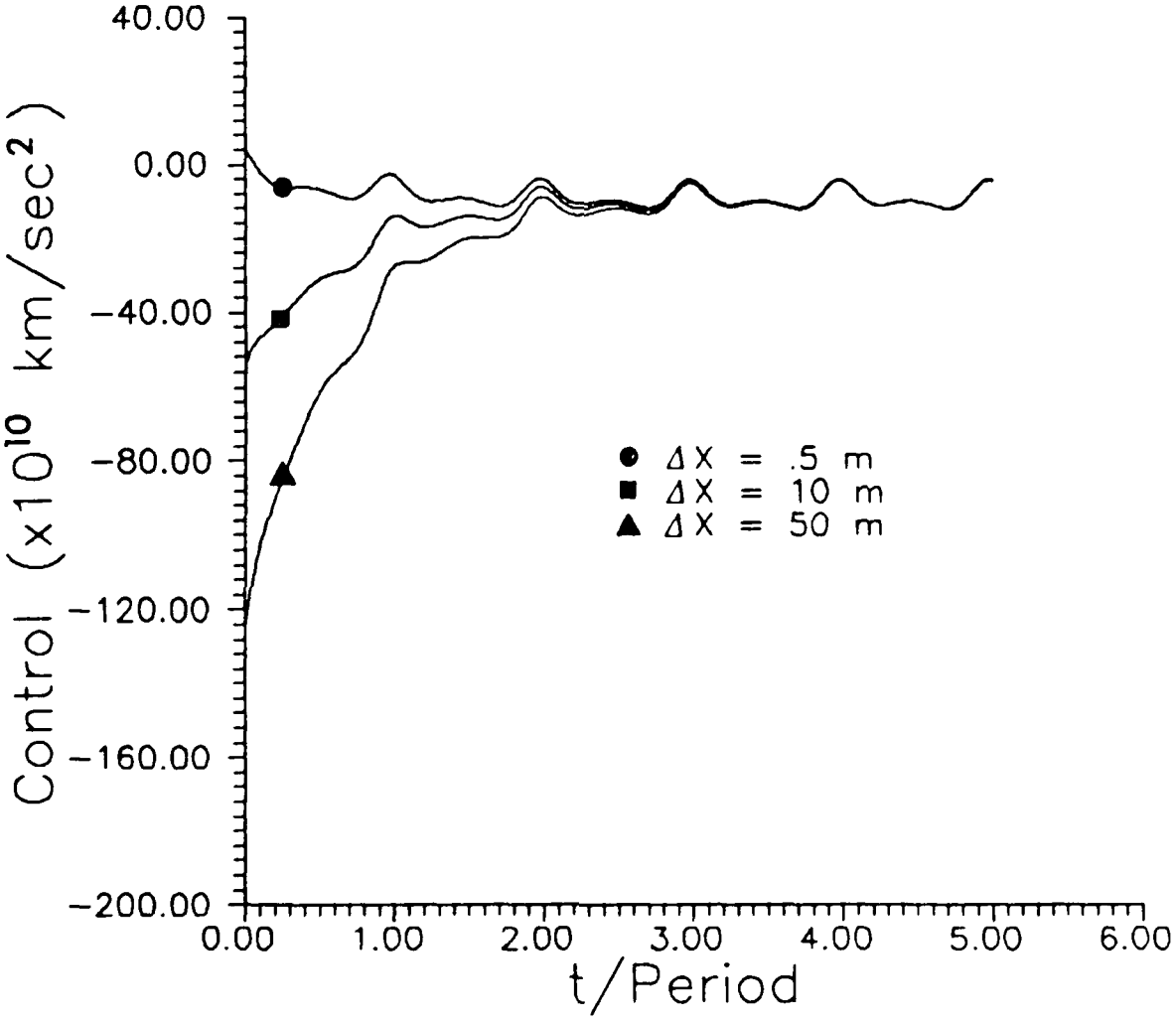

Figure 5: Control Thrust for Displacements in X

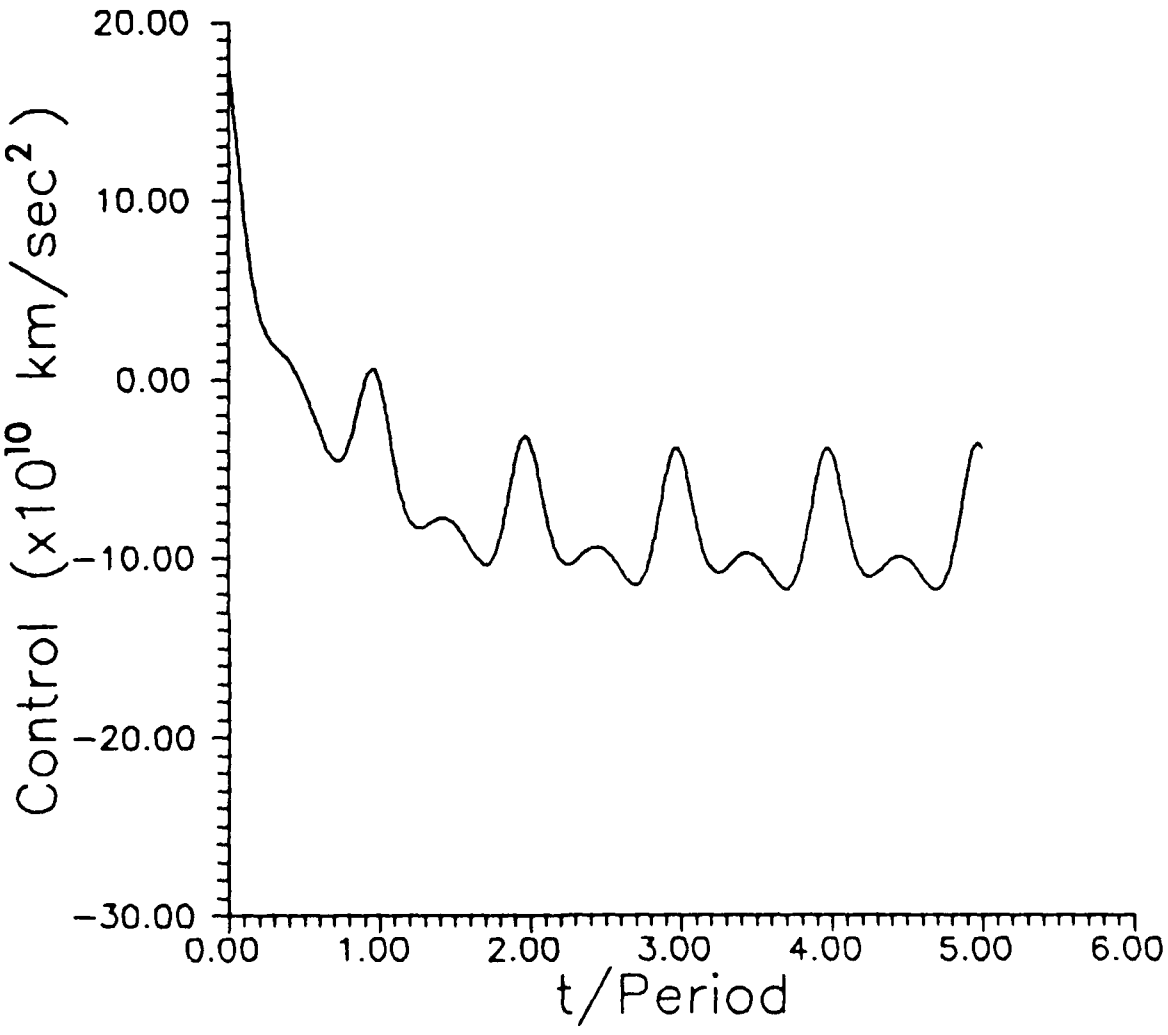

Figure 6: Control Thrust for Nominal Trajectory

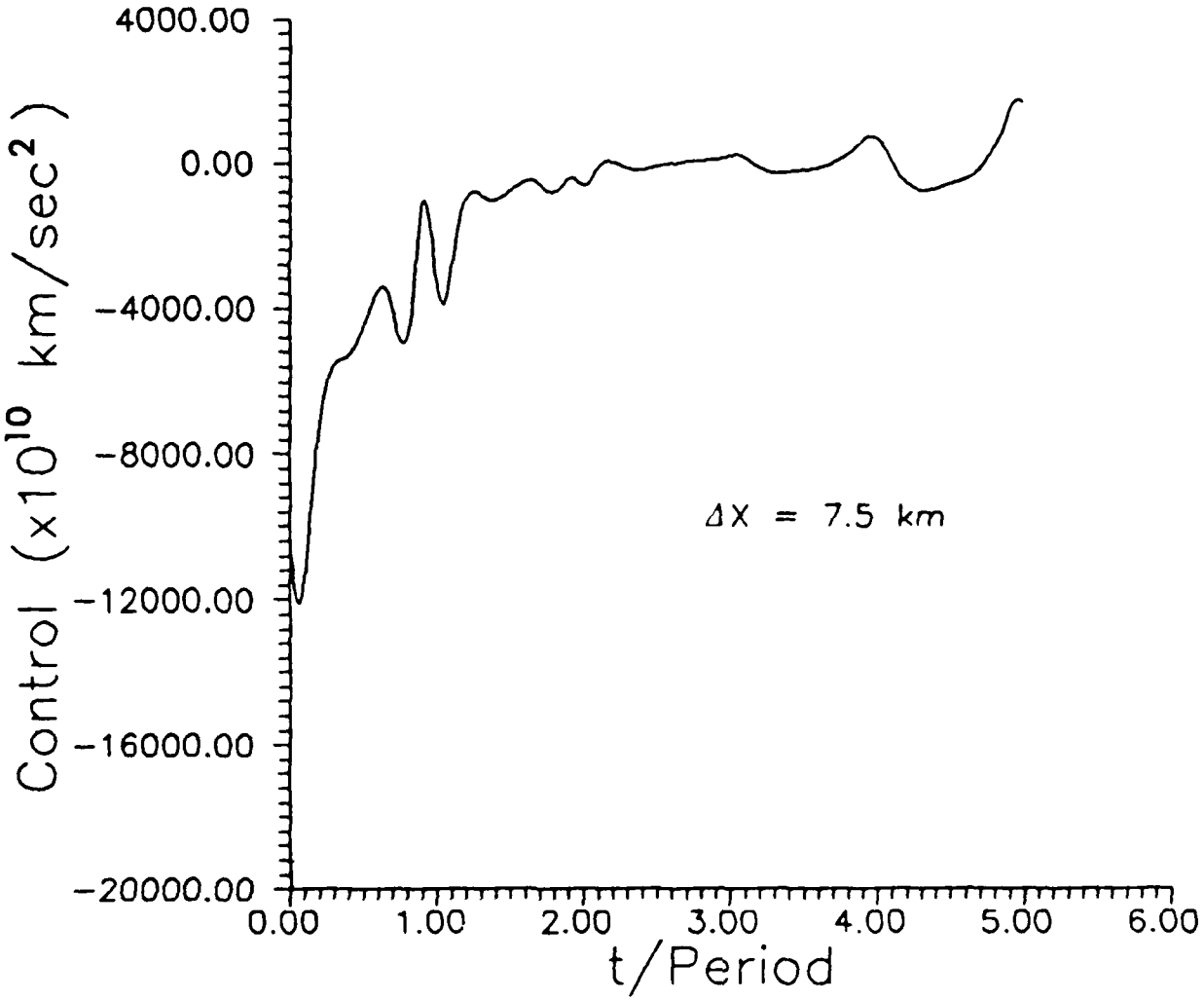

Figure 7: Nonlinear Control for Displacements in X

The control output was also investigated when the thrust was applied in the $\dot{P}_y$ direction. This is accomplished by setting [B] to

$$[B] = \begin{Bmatrix} 0 \\ 0 \\ 0 \\ 0 \\ 1 \\ 0 \end{Bmatrix} \tag{5-9}$$

The gain also needs to be recalculated using Equation (5-3) where g_{ic} is now the constant part of f_{is}^{-1}. The new gain is

$$k = 4.0188e\text{-}05 \tag{5-10}$$

The resulting control plots were similar to the plots presented above. However, the region of control instability changed, as shown in Table VI.

Table V: Displacements Which Produce Unstable Control in $\dot{P}_y$ Direction

ΔX : 10 m	ΔP_x : .5 cm/sec
ΔY : 10 m	ΔP_y : .5 cm/sec

VI. Conclusions and Recommendations

Periodic orbits about Phobos' equatorial plane have been located and discovered to be inherently unstable. These orbits may be stabilized by adding a control system which will shift the unstable Poincaré to the left hand plane. When the control system is implemented in the $\dot{P}_x$ direction, the amount of displacement away from the nominal trajectory which can be controlled successfully is greater than if the control were in the $\dot{P}_y$ direction. Therefore, putting the control system in the $\dot{P}_x$ direction would be more beneficial.

A possible extension of this research would be to investigate other types of orbits around Phobos to determine their stability and, if needed, controllability.

Appendix A: Problem Parameters

The following values were used when integrating the equations of motion and variation (6:35).

Phobos Axis Lengths

x = 10.8 km

y = 13.5 km

z = 9.4 km

(These values are used to compute the moments of inertia.)

Phobos' Orbital Radius

D = 9378 km

Phobos Rotation Rate

$\Omega = 2.28 \times 10^{-4}$ sec^{-1}

$GM_{Phob} = 6.6 \times 10^{-4}$ km^3/sec^2

$GM_{Mars} = 42828.32$ km^3/sec^2

Appendix B: Equations of Motion

The equations of motion were derived in Section II, and are listed here for reference.

$$\dot{X} = \frac{\partial H}{\partial P_x} = P_x + \Omega(Y - D) \qquad (2\text{–}36a)$$

$$\dot{Y} = \frac{\partial H}{\partial P_x} = P_y - \Omega X \qquad (2\text{–}36b)$$

$$\dot{Z} = \frac{\partial H}{\partial P_z} = P_z \qquad (2\text{-}36c)$$

$$\dot{P}_x = -\frac{\partial H}{\partial X} = \Omega P_y - \frac{GMmars}{D}\left[\frac{X}{D^2} - \frac{3XY}{D^3} - \frac{3R^2X}{2D^4}\right] - \frac{GMphobX}{R^3}$$

$$+ \frac{3GIX}{4R^5} - \frac{3GX}{4R^7}\left[(5X^2 - 2R^2)(I - 2I_{xx})\right.$$

$$\left. + 5Y^2(I - I_{yy}) + 5Z^2(I - I_{zz})\right] \qquad (2\text{–}36d)$$

$$\dot{P}_y = -\frac{\partial H}{\partial Y} = -\Omega P_x - \frac{GM_{mars}}{D}\left[\frac{1}{D} - \frac{4Y}{D^2}\,\frac{3(YR^2 - DR^2 - 2DY^2)}{2D^4}\right]$$

$$- \frac{GM_{phob}Y}{R^3} + \frac{3GIY}{4R^5} - \frac{3GY}{4R^7}\Big[5X^2(I - 2I_{xx})$$

$$+ (5Y^2 - 2R^2)(I - I_{yy}) + 5Z^2(I - I_{zz})\Big] \qquad (2\text{-}36e)$$

$$\dot{P}_z = -\frac{\partial H}{\partial Z} = -\frac{GM_{mars}}{D}\left[\frac{Z}{D^2} - \frac{3YZ}{D^3} - \frac{3R^2Z}{2D^4}\right] - \frac{GM_{phob}Z}{R^3}$$

$$+ \frac{3GIZ}{4R^5} - \frac{3GZ}{4R^7}\Big[5X^2(I - 2I_{xx})$$

$$+ 5Y^2(I - I_{yy}) + (5Z^2 - 2R^2)(I - I_{zz})\Big] \qquad (2\text{-}36f)$$

Appendix C: Equations of Variation

The equations of variation are defined as (See Section III)

$$[A(t)] = \left.\frac{\partial f}{\partial X}\right|_{xo} \qquad (3\text{–}8)$$

Therefore, [A(t)] has the form

$$[A(t)] = \begin{bmatrix} 0 & \Omega & 0 & 1 & 0 & 0 \\ -\Omega & 0 & 0 & 0 & 1 & 0 \\ 0 & 0 & 0 & 0 & 0 & 1 \\ A_{41} & A_{42} & A_{43} & 0 & \Omega & 0 \\ A_{51} & A_{52} & A_{53} & -\Omega & 0 & 0 \\ A_{61} & A_{62} & A_{63} & 0 & 0 & 0 \end{bmatrix} \qquad (C\text{–}1)$$

The elements for the lower left block are listed below.

$$A_{41} = -\frac{GM_{Mars}}{D^3}\left[1 - \frac{3Y}{D} + \frac{3(2X^2 + R^2)}{2D^2}\right]$$

$$-\frac{GM_{Phob}(R^2 - 3X^2)}{R^5} + \frac{3GI(R^2 - 5X^2)}{4R^7}$$

$$+\frac{3G}{4R^9}\Big[\left(2R^4 - 25X^2R^2 + 35X^4\right)\left(I - 2I_{xx}\right)$$

$$+ 5\left(7X^2 - R^2\right)\left(Y^2(I - 2I_{yy}) + Z^2(I - 2I_{zz})\right)\Big] \qquad (C\text{–}2)$$

$$A_{42} = -\frac{3GM_{Mars}X(Y-D)}{D^5} + \frac{3GM_{Phob}XY}{R^5} - \frac{15GXYI}{4R^7}$$

$$+ \frac{15GXY}{4R^9}\Big[\left(7X^2 - 2R^2\right)\left(I - 2I_{xx}\right)$$

$$+ \left(7Y^2 - 2R^2\right)\left(I - 2I_{yy}\right) + 7Z^2\left(I - 2I_{zz}\right) \Big] \qquad (C-3)$$

$$A_{43} = -\frac{3GM_{Mars}XZ}{D^5} + \frac{3GM_{Phob}XZ}{R^5} - \frac{15GXZI}{4R^7}$$

$$+ \frac{15GXZ}{4R^9}\Big[\left(7X^2 - 2R^2\right)\left(I - 2I_{xx}\right)$$

$$+ 7Y^2\left(I - 2I_{yy}\right) + \left(7Z^2 - 2R^2\right)\left(I - 2I_{zz}\right) \Big] \qquad (C-4)$$

$$A_{51} = A_{42} \qquad (C-5)$$

$$A_{sz} = -\frac{GM_{Mars}}{D^3}\left[4 + \frac{3(2Y^2 + R^2 - 6DY)}{2D^2}\right]$$

$$-\frac{GM_{Phob}(R^2 - 3Y^2)}{R^5} + \frac{3GI(R^2 - 5Y^2)}{4R^7}$$

$$+\frac{3G}{4R^9}\Big[\left(2R^4 - 25Y^2R^2 + 35Y^4\right)\left(I - 2I_{yy}\right)$$

$$+ 5\left(7Y^2 - R^2\right)\left(X^2(I - 2I_{xx}) + Z^2(I - 2I_{zz})\right)\Big] \qquad (C-6)$$

$$A_{sy} = -\frac{3GM_{Mars}Z(Y - D)}{D^5} + \frac{3GM_{Phob}YZ}{R^5} - \frac{15GYZI}{4R^7}$$

$$+\frac{15GYZ}{4R^9}\Big[\left(7Y^2 - 2R^2\right)\left(I - 2I_{yy}\right)$$

$$+ \left(7Z^2 - 2R^2\right)\left(I - 2I_{zz}\right) + 7X^2\left(I - 2I_{xx}\right)\Big] \qquad (C-7)$$

$$A_{c1} = A_{s3} \qquad (C-8)$$

$$A_{c2} = A_{s3} \qquad (C-9)$$

$$A_{cs} = -\frac{GM_{Mars}}{D^3}\left[1 - \frac{3Y}{D} + \frac{3(2Z^2 + R^2)}{2D^2}\right]$$

$$- \frac{GM_{Phob}(R^2 - 3Z^2)}{R^5} + \frac{3GI(R^2 - 5Z^2)}{4R^7}$$

$$+ \frac{3G}{4R^9}\Big[\left(2R^4 - 25Z^2R^2 + 35Z^4\right)\left(I - 2I_{zz}\right)$$

$$+ 5\left(7Z^2 - R^2\right)\left(X^2(I - 2I_{xx}) + Y^2(I - 2I_{yy})\right)\Big] \qquad (C-10)$$

Appendix D: Fourier Coefficients for $[F(t)]^{-1}$

Table D.1: Fourier Coefficients for f_{11}^{-1}

n	Cn	Sn
0	-3.874357399e-03	...
1	-8.783757104e-05	-1.328999018e-03
2	-1.243672401e-03	-3.070784026e-03
3	-5.804328285e-04	-1.177822744e-03
4	-1.869473398e-04	-3.495882023e-04
5	-7.482296244e-05	-1.309451163e-04
6	-2.281366727e-05	-3.141444948e-05
7	3.760515418e-06	1.266868843e-05
8	7.385247274e-06	1.421409351e-05
9	2.968862555e-06	4.589127202e-06
10	7.251091917e-08	-3.653094817e-07
11	-4.411260392e-07	-8.744324045e-07
12	-1.887865151e-07	-2.955821838e-07
13	-1.077366288e-08	9.315925218e-09
14	2.144612242e-08	4.433207188e-08

Table D.2: Fourier Coefficients for f_{12}^{-1}

n	Cn	Sn
0	2.117141101e-03	...
1	-2.690985867e-03	2.112497840e-04
2	-3.351871379e-03	1.321959626e-03
3	-1.218532650e-03	5.963226336e-04
4	-3.531718113e-04	1.886112093e-04
5	-1.282589944e-04	7.345863939e-05
6	-2.970104128e-05	2.185137305e-05
7	1.293546998e-05	-3.956126948e-06
8	1.405638000e-05	-7.316221724e-06
9	4.491670339e-06	-2.913765605e-06
10	-3.787635008e-07	-6.090322784e-08
11	-8.666678737e-07	4.377670807e-07
12	-2.915098603e-07	1.865378556e-07
13	1.020514649e-08	9.937113411e-09
14	4.371256120e-08	-2.134858245e-08

Table D.3: Fourier Coefficients for f_{13}^{-1}

n	Cn	Sn
0	0.000000000e+00	...
1	0.000000000e+00	0.000000000e+00
2	0.000000000e+00	0.000000000e+00
3	0.000000000e+00	0.000000000e+00
4	0.000000000e+00	0.000000000e+00
5	0.000000000e+00	0.000000000e+00
6	0.000000000e+00	0.000000000e+00
7	0.000000000e+00	0.000000000e+00
8	0.000000000e+00	0.000000000e+00
9	0.000000000e+00	0.000000000e+00
10	0.000000000e+00	0.000000000e+00
11	0.000000000e+00	0.000000000e+00
12	0.000000000e+00	0.000000000e+00
13	0.000000000e+00	0.000000000e+00
14	0.000000000e+00	0.000000000e+00

Table D.4: Fourier Coefficients for f_{14}^{-1}

n	Cn	Sn
0	1.432441162e+01	...
1	2.892993840e+00	-6.000430481e-01
2	2.455985030e+00	7.010133811e-01
3	-5.866175316e-01	2.420906168e-01
4	-1.262025226e-01	5.984262457e-02
5	-3.703386356e-02	1.933474339e-02
6	-7.328771575e-03	4.979233267e-03
7	2.485946774e-03	-6.673750133e-04
8	2.431689468e-03	-1.193868915e-03
9	6.990636181e-04	-4.279496821e-04
10	-5.303379851e-05	-1.397491958e-05
11	-1.067925343e-04	5.208135638e-05
12	-3.483747338e-05	2.322632631e-05
13	8.465511473e-07	-2.656660668e-06
14	3.572232102e-06	1.003728450e-06

Table D.5: Fourier Coefficients for f_{15}^{-1}

n	Cn	Sn
0	-8.385572830e+00	...
1	-6.634642137e-01	4.254127680e+00
2	7.328663541e-01	2.618125520e+00
3	2.474867601e-01	6.030240737e-01
4	6.029949451e-02	1.273106157e-01
5	1.902408885e-02	3.635979353e-02
6	4.792466561e-03	6.966502661e-03
7	-7.016951413e-04	-2.536812945e-03
8	-1.185650449e-03	-2.412165999e-03
9	-4.255307518e-04	-6.819834298e-04
10	-9.525491778e-06	5.256663100e-05
11	5.285072527e-05	1.071239763e-04
12	2.124386919e-05	3.215845265e-05
13	1.579965902e-06	-2.073022030e-06
14	-2.856467526e-06	-6.329853046e-06

Table D.6: Fourier Coefficients for $f_{1\sigma}^{-1}$

n	Cn	Sn
0	0.000000000e+00	...
1	0.000000000e+00	0.000000000e+00
2	0.000000000e+00	0.000000000e+00
3	0.000000000e+00	0.000000000e+00
4	0.000000000e+00	0.000000000e+00
5	0.000000000e+00	0.000000000e+00
6	0.000000000e+00	0.000000000e+00
7	0.000000000e+00	0.000000000e+00
8	0.000000000e+00	0.000000000e+00
9	0.000000000e+00	0.000000000e+00
10	0.000000000e+00	0.000000000e+00
11	0.000000000e+00	0.000000000e+00
12	0.000000000e+00	0.000000000e+00
13	0.000000000e+00	0.000000000e+00
14	0.000000000e+00	0.000000000e+00

Appendix E: Fourier Coefficients for X(t)

Table E.1: Fourier Coefficients for X

n	Cn	Sn
0	.883488e-11	...
1	.140728e-09	.152364e+02
2	.135547e-10	.649805e+00
3	.100078e-11	.544625e-01
4	.871430e-12	.949703e-02
5	-.127151e-12	.149213e-02
6	.598870e-13	-.765536e-03
7	-.247681e-13	-.561069e-03
8	-.545792e-13	-.127291e-03
9	.769867e-14	.166649e-04
10	-.256899e-13	.192629e-04
11	-.505583e-13	.467848e-05
12	-.243318e-13	-.436199e-06
13	-.347421e-14	-.611304e-06
14	-.630388e-13	-.151512e-06

Table E.2: Fourier Coefficients for Y

n	Cn	Sn
0	.479096e+01	...
1	.182127e+02	-.169361e-09
2	.677786e+00	-.118613e-10
3	.551567e-01	.212204e-11
4	.928735e-02	.481067e-11
5	.139793e-02	.670131e-11
6	.774109e-03	.821775e-11
7	.554801e-03	.965711e-11
8	.124648e-03	.110613e-10
9	.168713e-04	.124592e-10
10	.190833e-04	.138822e-10
11	.460648e-05	.152965e-10
12	.441411e-06	.167062e-10
13	.606409e-06	.181132e-10
14	.149646e-06	.195201e-10

Table E.3: Fourier Coefficients for Z

n	Cn	Sn
0	.000000e+00	...
1	.000000e+00	.000000e+00
2	.000000e+00	.000000e+00
3	.000000e+00	.000000e+00
4	.000000e+00	.000000e+00
5	.000000e+00	.000000e+00
6	.000000e+00	.000000e+00
7	.000000e+00	.000000e+00
8	.000000e+00	.000000e+00
9	.000000e+00	.000000e+00
10	.000000e+00	.000000e+00
11	.000000e+00	.000000e+00
12	.000000e+00	.000000e+00
13	.000000e+00	.000000e+00
14	.000000e+00	.000000e+00

Table E.4: Fourier Coefficients for P_x

n	C_n	S_n
0	.213928e+01	...
1	.752224e-02	.142745e-12
2	.841281e-03	.407597e-12
3	.112619e-03	.635699e-12
4	.269906e-04	.847254e-12
5	.539791e-05	.106258e-11
6	-.334303e-05	.127447e-11
7	-.288292e-05	.148699e-11
8	-.751878e-06	.170020e-11
9	.111064e-06	.191237e-11
10	.143236e-06	.212447e-11
11	.383699e-07	.233735e-11
12	-.392334e-08	.254974e-11
13	-.596416e-08	.276121e-11
14	-.160432e-08	.297555e-11

Table E.5: Fourier Coefficients for Py

n	Cn	Sn
0	.249991e-14	...
1	-.978226e-13	-.104815e-01
2	-.183950e-13	-.890540e-03
3	-.363208e-14	-.114373e-03
4	-.125753e-14	-.263001e-04
5	-.253473e-15	-.501555e-05
6	.117735e-15	.338438e-05
7	.148175e-15	.284786e-05
8	.247384e-16	.735059e-06
9	-.599974e-16	-.112549e-06
10	-.651474e-16	-.141833e-06
11	-.537480e-16	-.377605e-07
12	-.552417e-16	.395848e-08
13	-.593738e-16	.590029e-08
14	-.492293e-16	.156984e-08

Table E.6: Fourier Coefficients for P_z

n	C_n	S_n
0	.000000e+00	...
1	.000000e+00	.000000e+00
2	.000000e+00	.000000e+00
3	.000000e+00	.000000e+00
4	.000000e+00	.000000e+00
5	.000000e+00	.000000e+00
6	.000000e+00	.000000e+00
7	.000000e+00	.000000e+00
8	.000000e+00	.000000e+00
9	.000000e+00	.000000e+00
10	.000000e+00	.000000e+00
11	.000000e+00	.000000e+00
12	.000000e+00	.000000e+00
13	.000000e+00	.000000e+00
14	.000000e+00	.000000e+00

Appendix F: Graphical Results

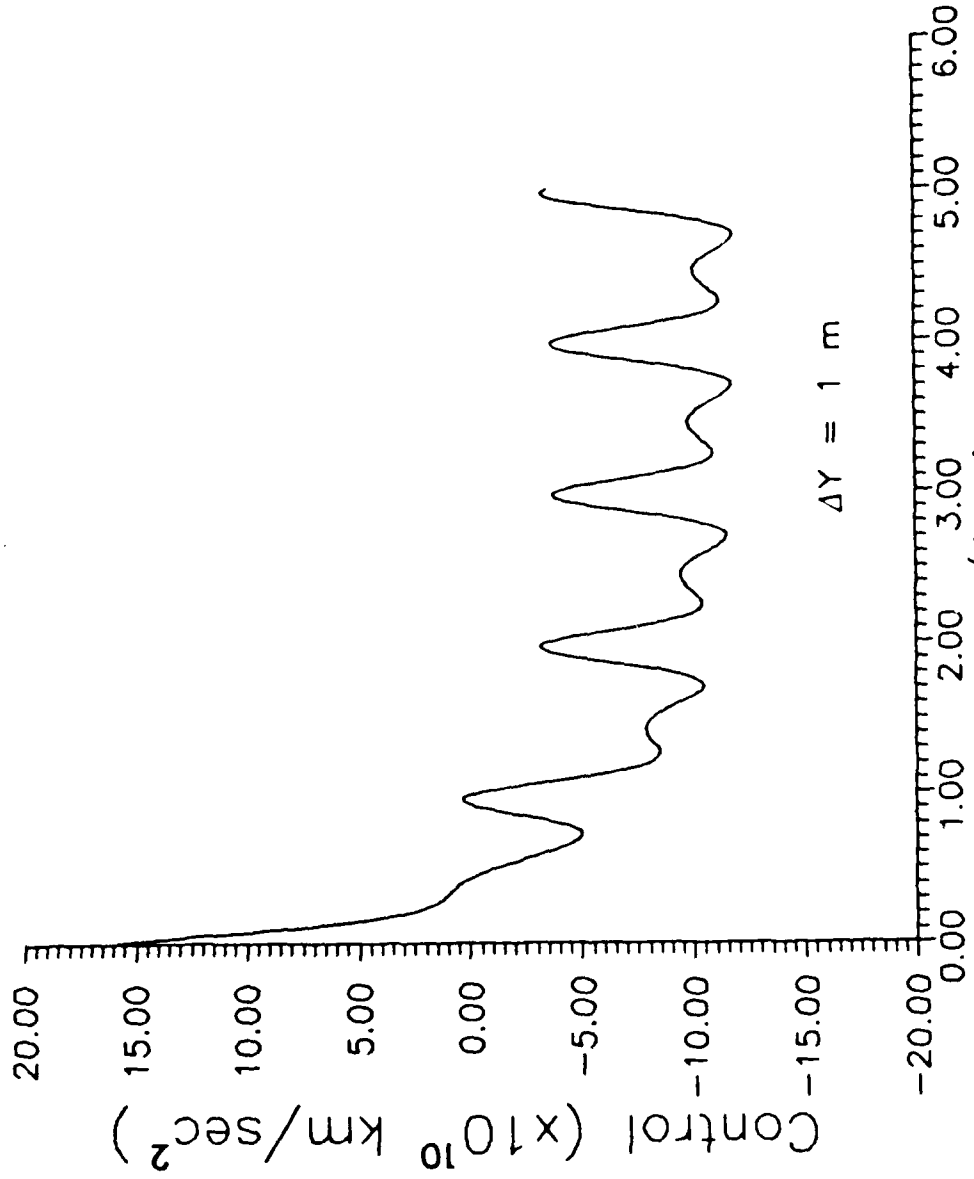

Figure F.1: Control Thrust for Displacements in Y

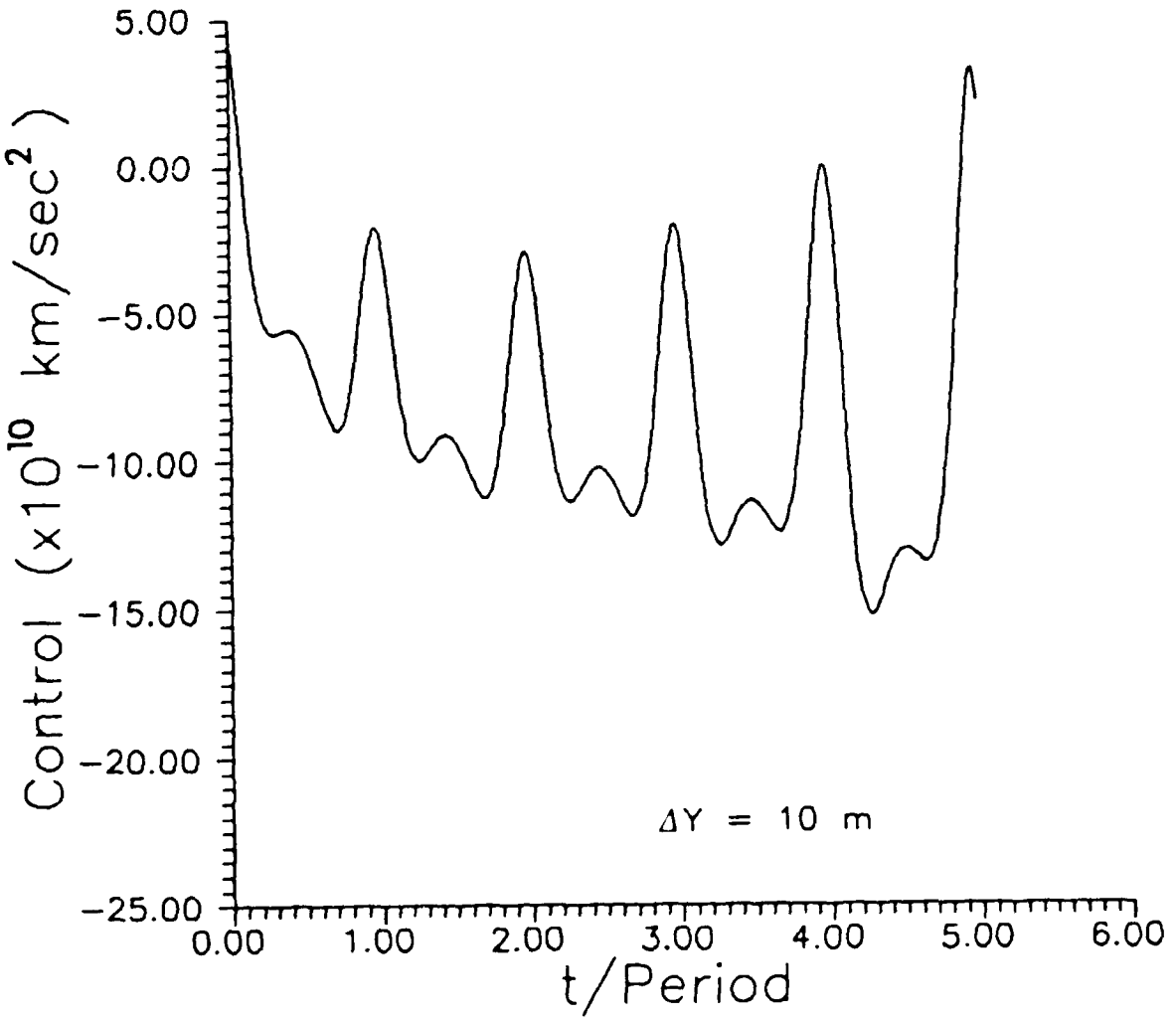

Figure F.2: Nonlinear Control for Displacements in Y

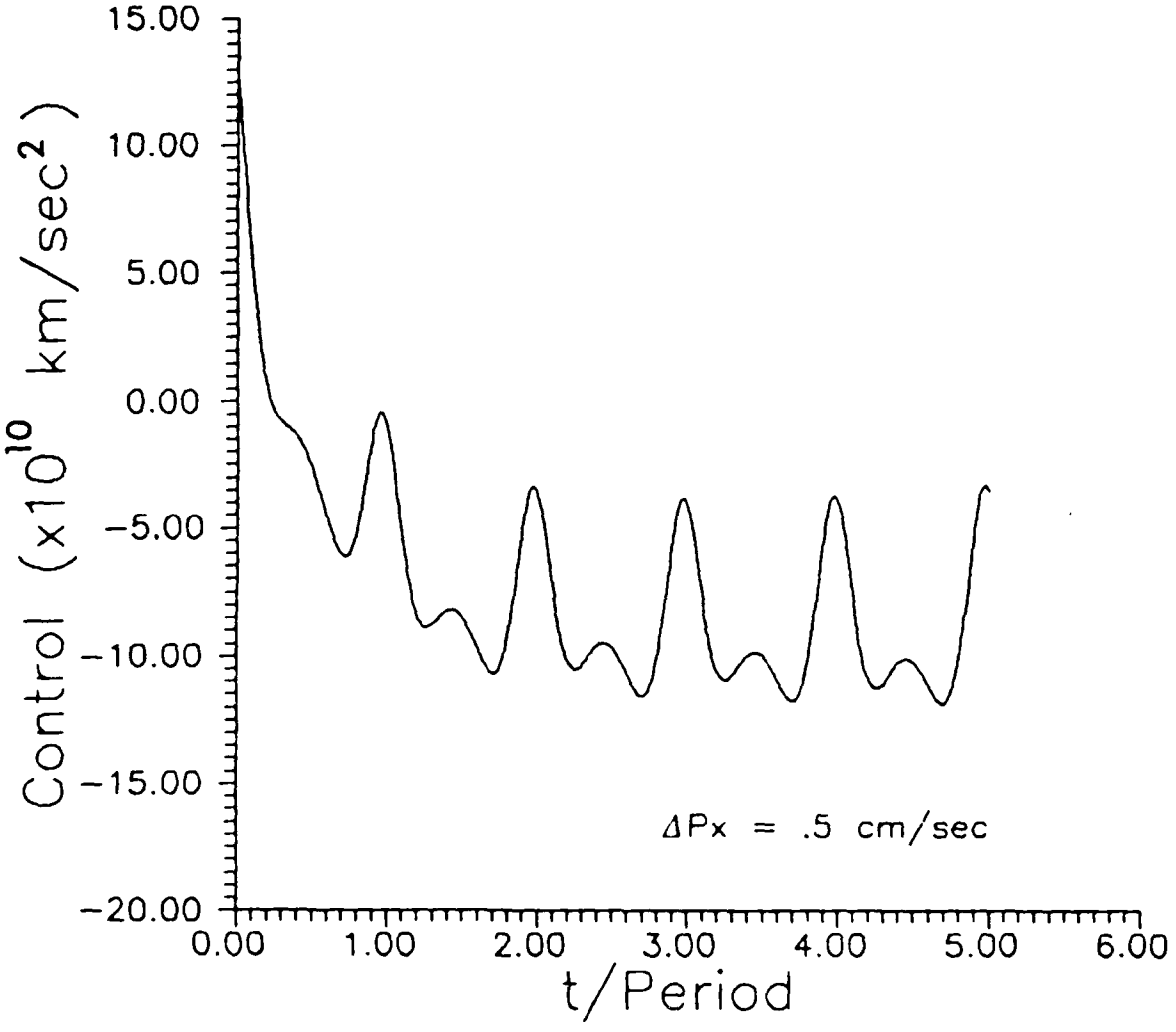

Figure F.3: Control Thrust for Displacements in Px

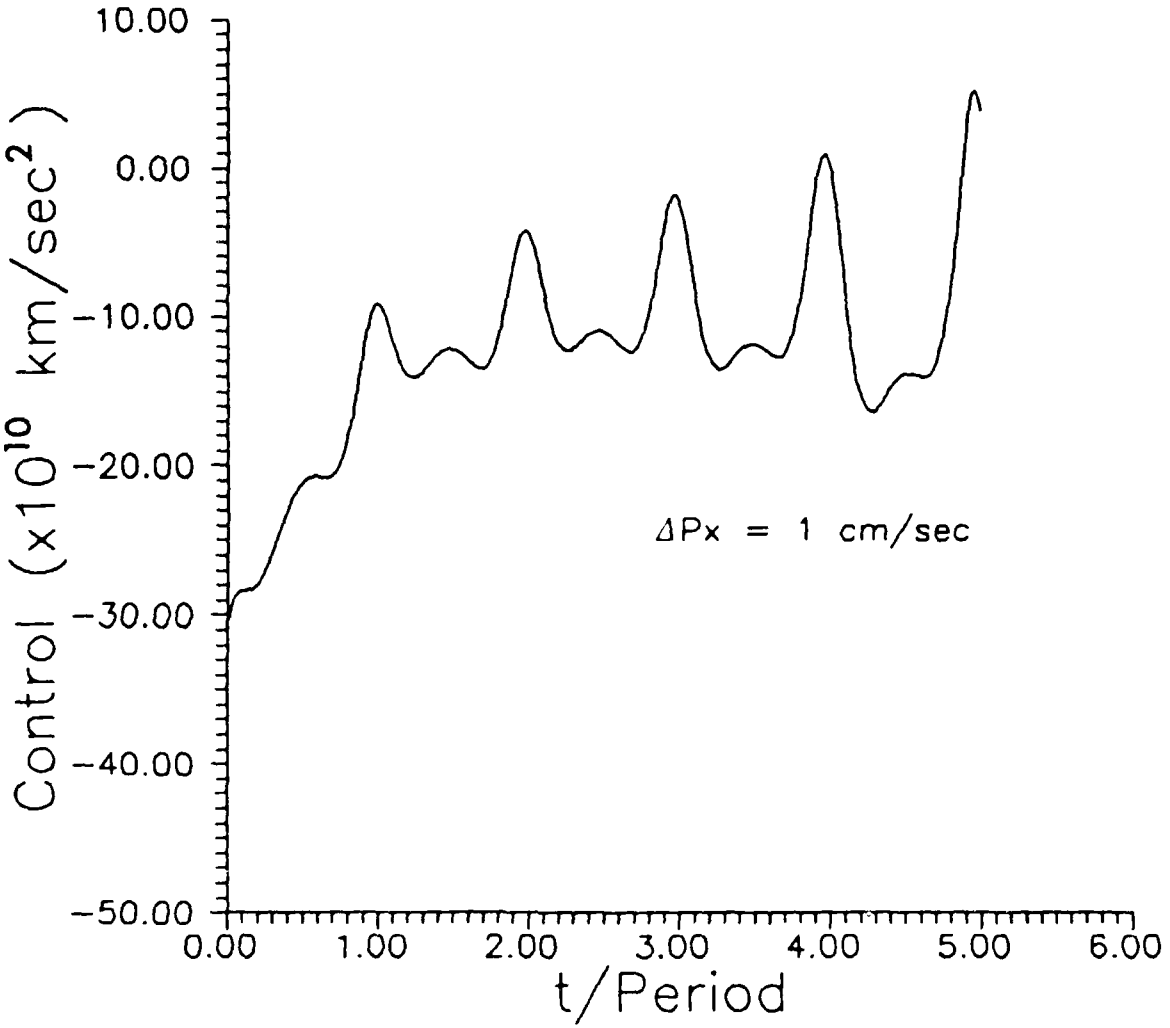

Figure F.4: Nonlinear Control for Displacements in Px

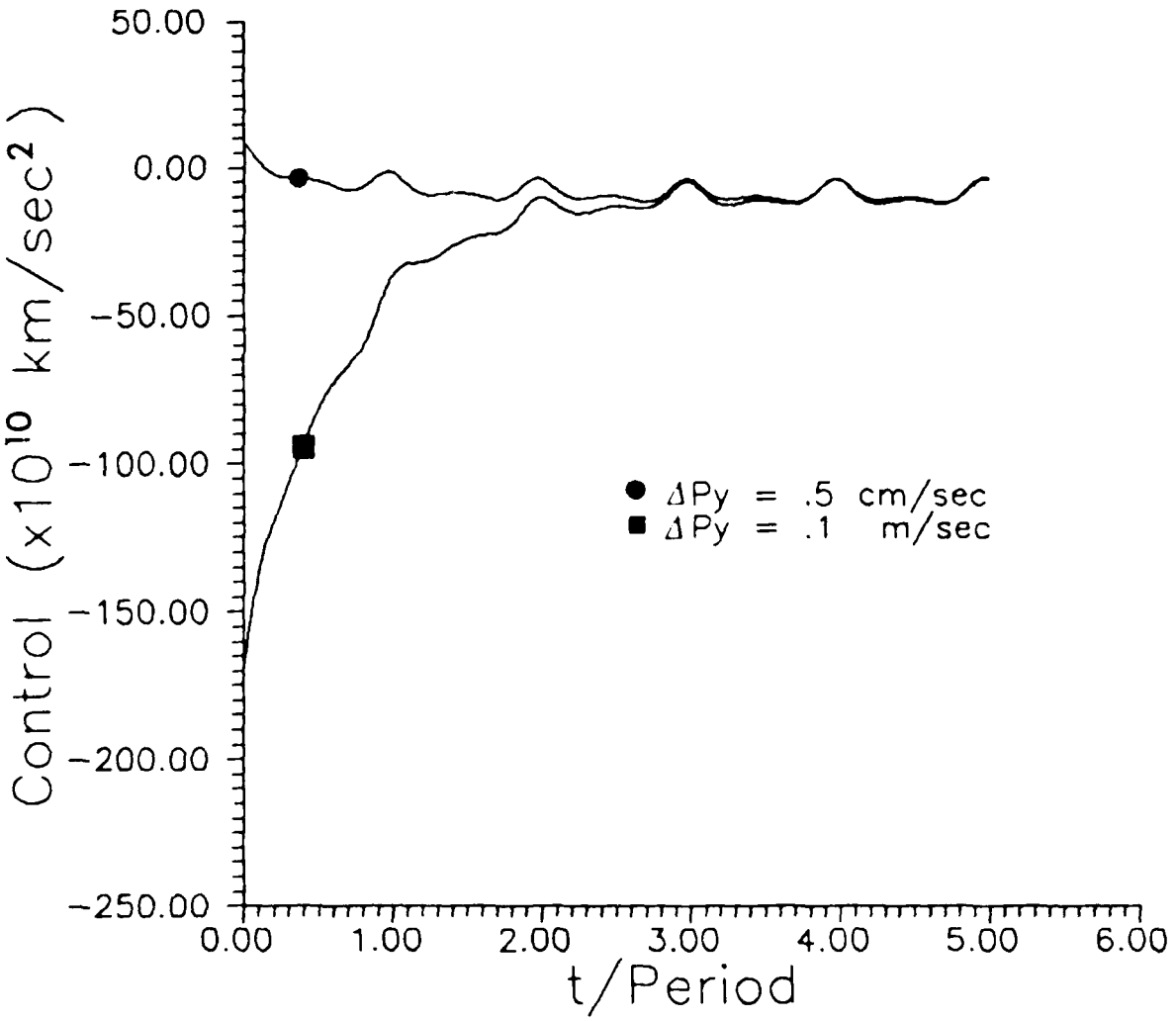

Figure F.5: Control Thrust for Displacements in Py

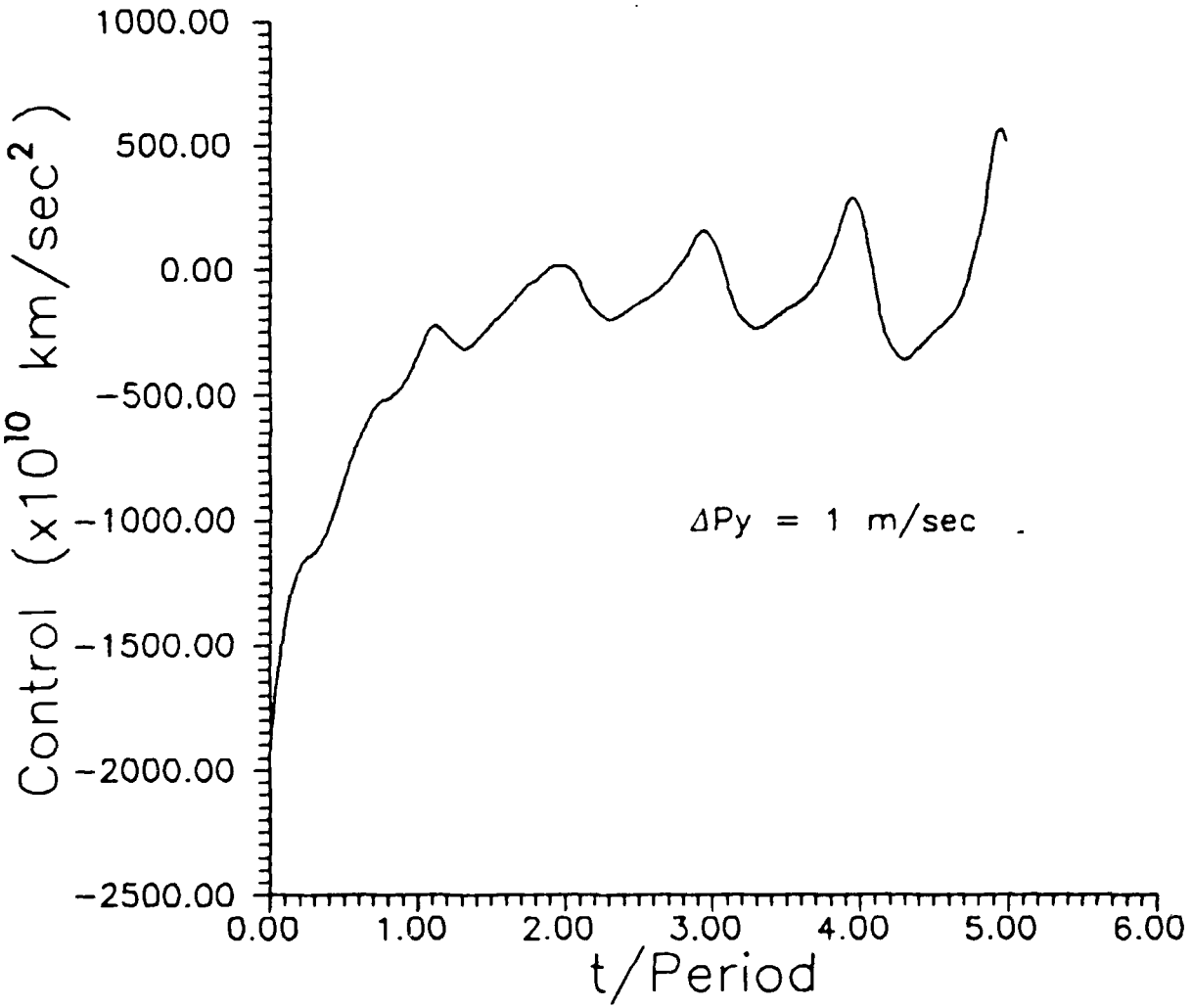

Figure F.6: Nonlinear Control for Displacements in Py

Bibliography

1. Brouwer, Dirk and Clemence, Gerald M. Methods of Celestial Mechanics. New York: Academic Press, 1961.

2. Calico, Robert A. and Wiesel William E. "Control of Time-Periodic Systems," Journal of Guidance, Control, and Dynamics, 7: 671-676 (November-December 1984).

3. Hicks, 2Lt Kerry D. Periodic Orbits About Rotating Asteriods in Free Space. MS Thesis, AFIT/GA/AA/86D-7. School of Engineering, Air Force Institute of Technology (AU), Wright Patterson AFB OH, December 1986.

4. Meintel, 2Lt James M. Relative Motion of Two Satellites in Close Elliptical Orbits. MS Thesis, AFIT/GA/AA/87D-8. School of Engineering, Air Force Institute of Technology (AU), Wright Patterson AFB OH, December 1987.

5. Meirovitch, Leonard Methods of Analytical Dynamics New York: McGraw-Hill Book Company, 1970.

6. Werner, Capt Rodney A. Periodic Orbits Around a Satellite Modelled as a Triaxial Ellipsoid. MS Thesis, AFIT/GA/AA/87D-8. School of Engineering, Air Force Institute of Technology (AU), Wright Patterson AFB OH, December 1987.

7. Wiesel, W. and Shelton, W. "Modal Control of an Unstable Periodic Orbit," Journal of the Astronautical Sciences, 31: 63-76 (January-March 1983).

8. Wiesel, W. Lecture Notes for MC636, Advanced Astrodynamics. School of Engineering, Air Force Institute of Technology (AU), Wright Patterson AFB OH, January 1987.

VITA

Captain Mary K. Solomon was born on [redacted] She graduated from [redacted] High School [redacted] 1980. She received her commission and her degree of Bachelor of Science in Electrical Engineering from the U.S. Air Force Academy in 1984. Her first assignment was to the 1st Strategic Aerospace Division, Test and Evaluation Deputate, where she worked on the Peacekeeper missile system as the Assistant Chief, Advanced ICBM Electrical Systems Branch, and as the Advanced ICBM Test Program Engineer. Captain Solomon entered the Air Force Institute of Technology, School of Engineering, in June of 1987.

[redacted]

SECURITY CLASSIFICATION OF THIS PAGE

REPORT DOCUMENTATION PAGE

Form Approved
OMB No. 0704-0188

1a. REPORT SECURITY CLASSIFICATION UNCLASSIFIED	1b. RESTRICTIVE MARKINGS
2a. SECURITY CLASSIFICATION AUTHORITY	3. DISTRIBUTION / AVAILABILITY OF REPORT Approved for public release; distribution unlimited
2b. DECLASSIFICATION / DOWNGRADING SCHEDULE	
4. PERFORMING ORGANIZATION REPORT NUMBER(S) AFIT/GA/AA/88D-10	5. MONITORING ORGANIZATION REPORT NUMBER(S)
6a. NAME OF PERFORMING ORGANIZATION School of Engineering 6b. OFFICE SYMBOL (If applicable) AFIT/EN	7a. NAME OF MONITORING ORGANIZATION
6c. ADDRESS (City, State, and ZIP Code) Air Force Institute of Technology Wright-Patterson AFB, Ohio 45433	7b. ADDRESS (City, State, and ZIP Code)
8a. NAME OF FUNDING / SPONSORING ORGANIZATION 8b. OFFICE SYMBOL (If applicable)	9. PROCUREMENT INSTRUMENT IDENTIFICATION NUMBER
8c. ADDRESS (City, State, and ZIP Code)	10. SOURCE OF FUNDING NUMBERS PROGRAM ELEMENT NO / PROJECT NO / TASK NO / WORK UNIT ACCESSION NO

11. TITLE (Include Security Classification)

Control System for Maintaining Stable Orbits Around Phobos

12. PERSONAL AUTHOR(S)

Mary K. Solomon, B.S.E.E., Capt, USAF

13a. TYPE OF REPORT	13b. TIME COVERED	14. DATE OF REPORT (Year, Month, Day)	15. PAGE COUNT
MS Thesis	FROM _____ TO _____	1988 December	84

16. SUPPLEMENTARY NOTATION

17. COSATI CODES			18. SUBJECT TERMS (Continue on reverse if necessary and identify by block number)
FIELD	GROUP	SUB-GROUP	Control Theory, Phobos, Orbits, Mars
22	3		

19. ABSTRACT (Continue on reverse if necessary and identify by block number)

Thesis Chairman: William E. Wiesel, Ph.D.
Professor of Astronautics

William E. Wiesel
12 Jan 1989

20. DISTRIBUTION / AVAILABILITY OF ABSTRACT	21. ABSTRACT SECURITY CLASSIFICATION
☐ UNCLASSIFIED/UNLIMITED ☒ SAME AS RPT ☐ DTIC USERS	UNCLASSIFIED
22a. NAME OF RESPONSIBLE INDIVIDUAL William E. Wiesel, Ph.D.	22b. TELEPHONE (Include Area Code) 513-255-2362 22c. OFFICE SYMBOL AFIT/EN

DD Form 1473, JUN 86 Previous editions are obsolete

SECURITY CLASSIFICATION OF THIS PAGE

UNCLASSIFIED

AFIT/GA/AA/88D-10

Abstract

Phobos can be modeled as a triaxial ellipsoid in a circular orbit around Mars. The orbital dynamics of a satellite in orbit around Phobos are derived using Hamilton's canonical equations. An algorithm is then developed to find closed orbits for a specified period. Periodic orbits in Phobos' orbital plane have been found to be unstable. A control system is developed using scalar modal control to stabilize the orbit by shifting the unstable Poincaré exponent to the left-half plane.